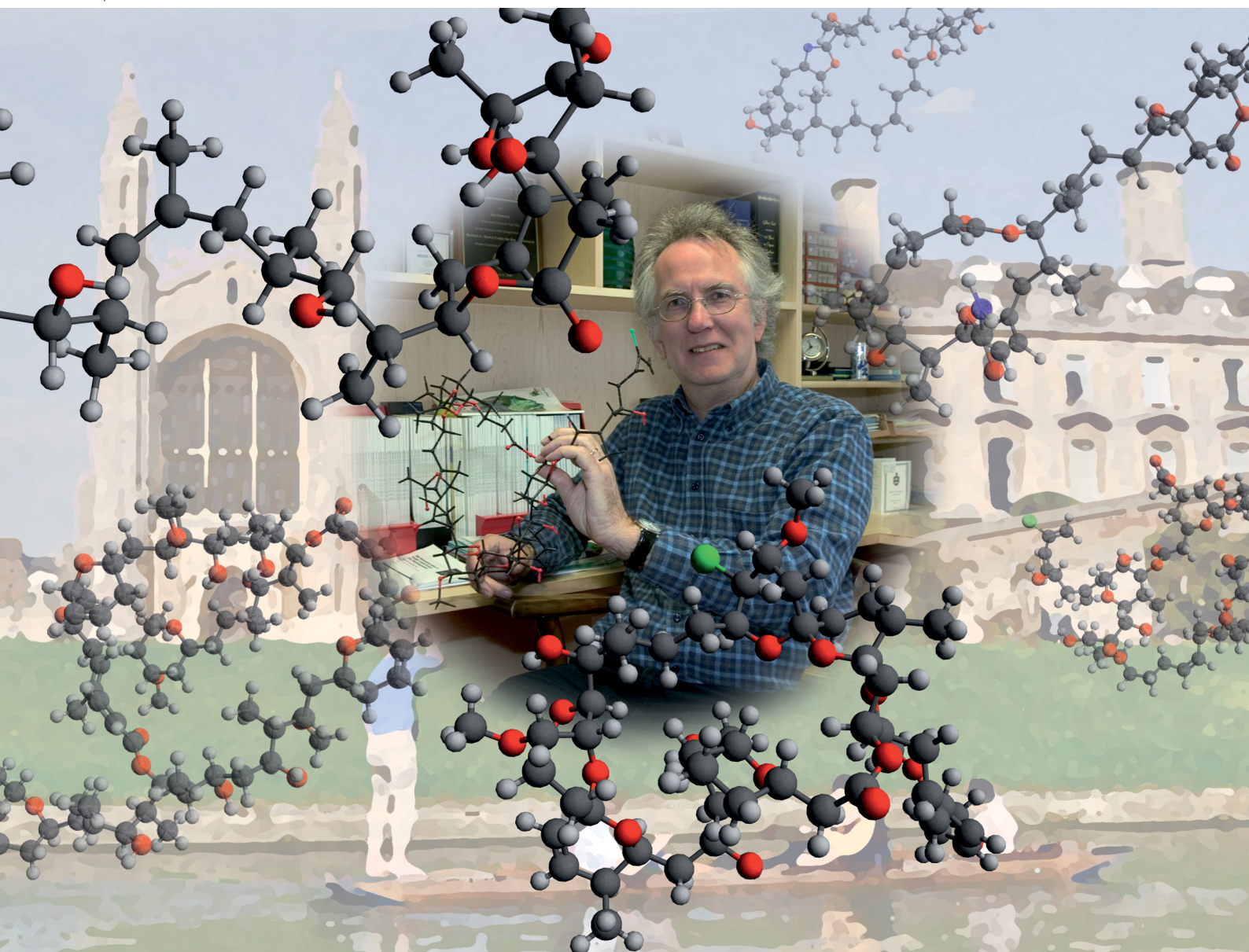


# ChemComm

Chemical Communications

[rsc.li/chemcomm](http://rsc.li/chemcomm)



ISSN 1359-7345

**FEATURE ARTICLE**

Ian Paterson *et al.*

Conquering peaks and illuminating depths: developing stereocontrolled organic reactions to unlock nature's macrolide treasure trove



Cite this: *Chem. Commun.*, 2021, 57, 3171

Received 25th January 2021,  
Accepted 23rd February 2021

DOI: 10.1039/d1cc00442e

rsc.li/chemcomm

# Conquering peaks and illuminating depths: developing stereocontrolled organic reactions to unlock nature's macrolide treasure trove

Nelson Y. S. Lam, <sup>†ab</sup> Tegan P. Stockdale,<sup>†a</sup> Matthew J. Anketell<sup>†a</sup> and Ian Paterson <sup>\*a</sup>

The structural complexity and biological importance of macrolide natural products has inspired the development of innovative strategies for their chemical synthesis. With their dense stereochemical content, high level of oxygenation and macrocyclic cores, we viewed the efficient total synthesis of these valuable compounds as an aspirational driver towards developing robust methods and strategies for their construction. Starting out from the initial development of our versatile asymmetric aldol methodology, this personal perspective reflects on an adventurous journey, with all its trials, tribulations and serendipitous discoveries, across the total synthesis, in our group, of a representative selection of six macrolide natural products of marine and terrestrial origin – swinholide A, spongistatin 1, spirastrellolide A, leiodermatolide, chivosazole F and actinoallolide A.

## 1. Introduction

The varied landscape of nature has shaped the evolution of a range of organisms large and small. Through their adaptations, which are fundamentally chemical in origin, they have developed intricate mechanisms to survive and thrive. This has resulted in

the evolution of an equally diverse and varied landscape of natural products found within organisms that live from the highest mountains down to the deepest ocean trenches. Compared to nature's timescale, humanity's ability to manipulate the chemical world stands as a miniscule flash of time, differing by over six orders of magnitude! And yet in the last 200 years, the staggering advances made across the chemical sciences have produced powerful synthetic tools to target the privileged chemical space that natural products occupy, giving an unmatched opportunity to exploit their biological function in drug discovery.<sup>1</sup>

Like artists inspired by the majesty of nature, we were drawn to the exquisite 3D form and function of these intricate natural

<sup>a</sup> Yusuf Hamied Department of Chemistry, University of Cambridge, Lensfield Road, Cambridge CB2 1EW, UK

<sup>b</sup> The Scripps Research Institute, 10550 N Torrey Pines Road, La Jolla, California, 92037, USA

<sup>†</sup> Authors contributed to this manuscript equally.



Nelson Y. S. Lam

Nelson Lam received his BSc (Hons) degree (2015) from the University of Auckland, working in the lab of Prof. Christian Hartinger. He obtained his PhD at the University of Cambridge (2019) under the supervision of Prof. Ian Paterson as a Woolf Fisher Scholar, where he worked on the total synthesis of polyketide natural products. He is currently a postdoctoral associate and Lindemann Fellow with Prof. Jin-Quan Yu at the

Scripps Research Institute, developing novel Pd-catalysed C(sp<sup>3</sup>)-H functionalisation transformations.



Tegan P. Stockdale

Tegan Stockdale received her BSc (Hons) and LLB (Hons) degrees (2016) from the University of Queensland, working in the labs of Prof. James de Voss and Prof. Joanne Blanchfield on the bioavailability of steroidal saponin natural products, isolation of bioactive products from traditional medicinal plants and synthesis of mechanistic probe molecules for cytochrome P450 enzymes. She is currently pursuing her PhD at the University of Cambridge under the supervision

of Prof. Ian Paterson as a Herchel Smith Scholar, embarking on the total synthesis of the stereochemically-ambiguous natural product hemicalide.



products, with polyketides being one important bioactive class that proved particularly alluring. Belying their complex yet flexible molecular scaffolds, featuring characteristic oxygenation patterns and rich stereochemical detail, is a deceptively straightforward means for their biosynthesis engineered by polyketide synthases. This ubiquitous pathway has inspired the development of a similarly robust methodology for their total synthesis in the laboratory, generating a toolbox of stereoselective aldol reactions to replicate nature's biosynthetic machinery.

Over the last 30 years, these powerful molecular construction tools have enabled the successful completion of the total synthesis of over 40 bioactive polyketide natural products in our group. Throughout each journey, we have traversed diverse chemical terrains, with each synthetic campaign bringing its own unique set of challenges, rewards and new knowledge. Like an intrepid explorer fondly looking back on their most memorable adventures, this Feature Article recounts a personal selection of career highlights.<sup>2</sup> We chronicle the winding paths followed, hurdles overcome and lessons gleaned from the total synthesis of a select group of macrocyclic polyketides of marine and terrestrial origin: swinholide A (1994), spongistatin 1 (2001), spirastrellolide A methyl ester (2008, 2012), leiodermatolide (2014), chivosazole F (2017) and actinoallolide A (2020).

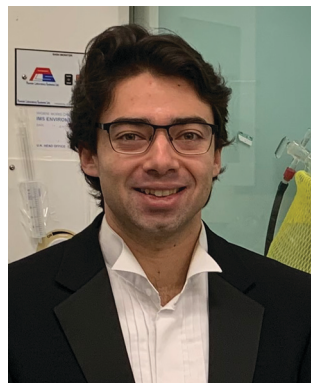
## 2. Asymmetric boron-mediated aldol methodology for the construction of complex polyketide natural products

To preface how we approached the total synthesis of these macrolide natural products, we must first introduce the toolbox of aldol reactions developed to enable the construction of

complex polyketide structures. The biosynthesis of complex polyketides is elegantly engineered by polyketide synthases. This operates *via* an iterative stepwise sequence of chain extension, based on a decarboxylative Claisen-like condensation and ketone reduction, to configure the vicinal methyl-bearing and carbinol stereocentres (Scheme 1).

In a laboratory setting, it was envisaged to replicate this process through a directed asymmetric aldol reaction between a methyl or ethyl ketone and aldehyde, setting one or two stereocentres in a diastereo- and/or enantioselective manner.<sup>3,4</sup> The resulting  $\beta$ -hydroxyketone can then undergo a controlled 1,3-*syn* or 1,3-*anti* reduction to configure up to three contiguous stereocentres.<sup>5</sup> These aldol-based bond constructions would then enable the controlled synthesis of diverse polyoxygenated chiral building blocks and facilitate the coupling of advanced fragments.<sup>6</sup> In contrast to the enforced linearity of the biosynthetic polyketide assembly lines, the chemical synthesis would also make possible the convergent construction of complex intermediates in total synthesis.

For the boron-mediated aldol reactions of ethyl ketones, the relative configuration of the methine and carbinol stereocentres principally arises from the selectivity of the initial enolisation step, where *Z*-enolates produce *syn*-adducts while *E*-enolates produce *anti*-adducts (Scheme 2).<sup>6</sup> In general, enolate geometry can be divergently controlled using a suitable combination of boron Lewis acid and tertiary amine base. Small ligands and a good leaving group on boron, combined with a bulky amine base (*e.g.* *n*Bu<sub>2</sub>BOTf, iPr<sub>2</sub>NEt), promote the selective formation of *Z*-enolates. Conversely, sterically demanding ligands and a poor leaving group on boron, combined with a small amine base (*e.g.* *c*Hex<sub>2</sub>BCL, Et<sub>3</sub>N), promote the selective formation of *E*-enolates.



**Matthew J. Anketell**

is currently a postdoctoral associate with Prof. Robert Britton at Simon Fraser University, Canada.

Matthew Anketell received his BA and MA from the University of Cambridge, reading the Natural Sciences Tripos. In 2015, he joined the Paterson group where he embarked on the synthesis of the stereochemically-ambiguous patellazole marine natural products. He then continued research in the same group as a Herchel Smith Scholar, where he completed the total synthesis of the actinoallolide class of anti-trypanosomal macrolides, to obtain his PhD (2020). He



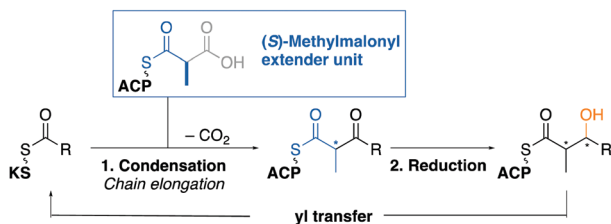
**Ian Paterson**

the University of St Andrews and PhD from the University of Cambridge, working with Prof. Ian Fleming. After a postdoctoral period with Prof. Gilbert Stork at Columbia University, he joined the faculty at University College London. In 1983, he returned to Cambridge, where he is Professor of Organic Chemistry and a Fellow of Jesus College. His research achievements have been recognised by various awards, and he is a Fellow of the Royal Society and the Royal Society of Edinburgh.

Ian Paterson's father was a master builder who shared with him the conviction that one of the best jobs you can do is a creative one, seeding his ambition to become a molecule maker. Enthralled by the aesthetic qualities of natural product structures and their biological function, his career has focused on the development of new synthetic methodology and its application in total synthesis to unlock nature's polyketide treasure trove. He received his BSc (Hons) degree from



## Polyketide biosynthesis via decarboxylative Claisen condensation and reduction

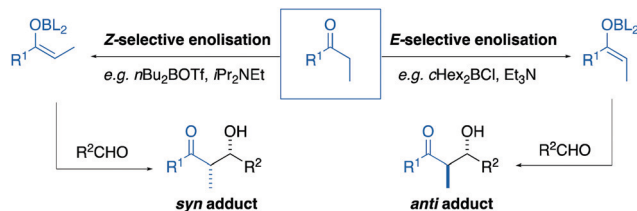


**Scheme 1** Overview of polyketide biosynthesis. Proposed replication by an asymmetric aldol addition coupled with a 1,3-*syn* or 1,3-*anti* β-hydroxyketone reduction to configure up to three stereocentres. ACP: acyl carrier protein; KS: ketosynthase unit.

Methyl ketones generally undergo regioselective enolisation to generate the less substituted enolate. For both methyl and ethyl ketones, the resulting boron enolates react with aldehydes through a highly-ordered six-membered cyclic transition state, which is sensitive to steric and electronic influences.<sup>4,7</sup>

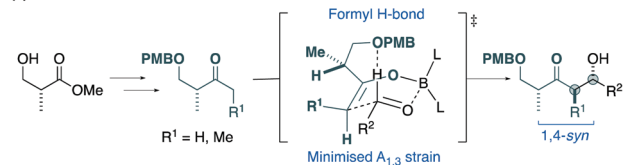
In developing asymmetric boron-mediated aldol methodology for complex polyketide synthesis (Scheme 3), we addressed achieving π-facial selectivity by: (a) substrate-based control, using a chiral enolate; (b) auxiliary-based control, using an enolate with a cleavable chiral directing group; (c) reagent-based control, arising from the steric influence of chiral ligands on boron.<sup>7</sup> We realised that the chiral pool Roche ester, which is commercially available in both enantiomeric forms, can be readily transformed into the corresponding methyl and ethyl ketones, enabling incorporation of a defined methyl-bearing stereocentre and reliable 1,4-*syn* selectivity in boron-mediated aldol reactions of type (a).<sup>8</sup>

Building on these findings, we next developed a set of lactate-derived ketones, which offer a complementary means of generating aldol adducts of type (b) that can be manipulated in various ways, including conversion into protected β-hydroxyaldehydes.<sup>9</sup> Finally, we pioneered the application of convenient Lewis acids bearing isopinocampheyl (Ipc) ligands on boron to asymmetric aldol reactions of type (c).<sup>7,10</sup> This important development allowed the

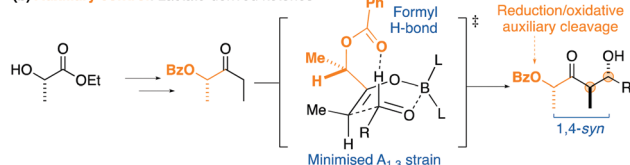


**Scheme 2** Diastereoselectivity in boron-mediated aldol reactions is determined by the geometric selectivity of the enolisation step.

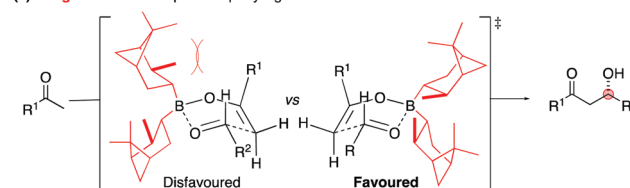
## (a) Substrate control: Roche ester-derived ketones



## (b) Auxiliary control: Lactate-derived ketones



## (c) Reagent control: Isopinocampheyl ligands on boron



**Scheme 3** Factors that govern π-facial selectivity in boron-mediated aldol reactions by imparting: (a) substrate control through the use of Roche ester-derived ketones; (b) auxiliary control through the use of lactate-derived ketones; (c) reagent control through the use of Ipc ligands on boron.

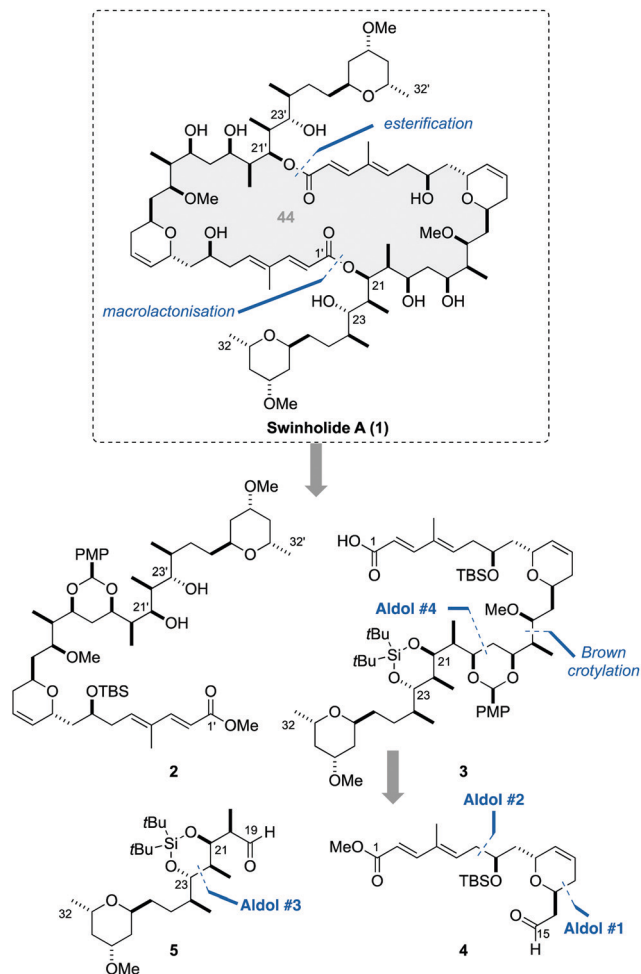
reinforcement or even the reversal of the intrinsic π-facial selectivity of the substrates, as well as enabling the practical synthesis of enantiomerically enriched aldol adducts from achiral ketone and aldehyde components. Collectively, these reliable and versatile construction tools afford controlled access to a diverse range of β-hydroxyketones, expediently addressing the synthetic challenges posed by macrolide and other polyketide natural products. In the remainder of this Article, the application of these reactions in total synthesis is showcased in the context of a representative selection of six bioactive macrolides completed in the group.

### 3. Total synthesis of bioactive macrolides enabled by aldol methodology

#### 3.1 Swinholide A

Swinholide A (1, Scheme 4) was first reported in 1985 by Carmely and Kashman, following its isolation from the marine sponge *Theonella swinhoei*.<sup>11</sup> Originally misassigned as a monomeric 22-membered macrolide, subsequent X-ray crystallographic analysis by the Kobayashi/Kitagawa group revealed the C<sub>2</sub>-symmetric, dimeric structure of this unusually large 44-membered macrodiolide and permitted the secure configurational assignment of the 30 stereocentres.<sup>12</sup> Swinholide A showed potent cytotoxicity across a number of cancer cell lines,<sup>13</sup> with actin determined to be its cytoskeletal target.<sup>14</sup> Interestingly, it shares a high degree of structural homology with various other macrolides of both marine and terrestrial origin, providing evidence for its production by symbiotic heterotrophic bacteria.<sup>15</sup>

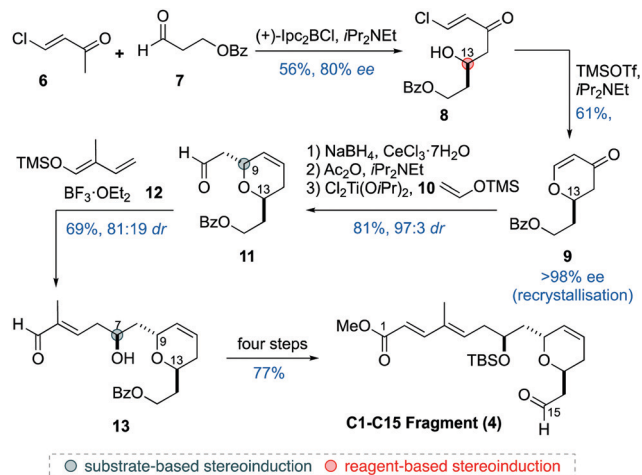




Scheme 4 Structure and retrosynthetic analysis of swinholide A (**1**), highlighting the four aldol disconnections.

Drawn by its intriguing molecular architecture and potent bioactivity, swinholide A was identified as an attractive target<sup>16</sup> to showcase the nascent aldol methodology developed in the group.<sup>17–24</sup> As such, this project stands out as an early career highlight. We developed a flexible modular strategy, where the related monomeric units **2** and **3** would be constructed from fragments **4** and **5**, while installation of the 44-membered macrodiolide relied on an adventurous site-selective esterification and macrocyclisation. This permitted two alternative sequences of fragment assembly to be explored to determine the optimum route. Four strategic aldol disconnections were identified as highlighted.

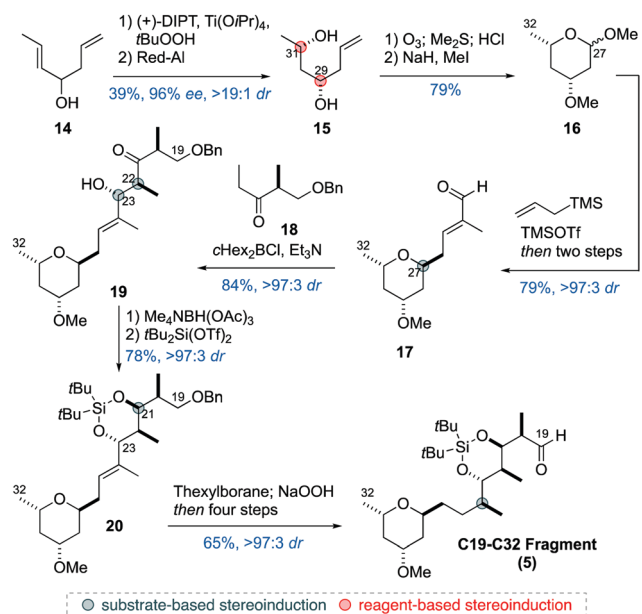
Preparation of C1–C15 aldehyde **4** commenced with the asymmetric construction of the dihydropyran ring (Scheme 5).<sup>17</sup> An (+)-Ipc<sub>2</sub>BCl-mediated aldol reaction between methyl ketone **6** and aldehyde **7** gave β-chloroenone **8**, which was cyclised to provide dihydropyranone **9**. Subsequent Luche reduction and Lewis acid-mediated alkylation of silyl enol ether **10** proceeded, *via* a Ferrier-type rearrangement, to afford aldehyde **11**. Next, a vinylogous Mukaiyama aldol reaction between silyl dienol ether **12** and aldehyde **11**, promoted by BF<sub>3</sub>·OEt<sub>2</sub>, selectively provided 1,3-*anti*



Scheme 5 Synthesis of C1–C15 aldehyde **4**.

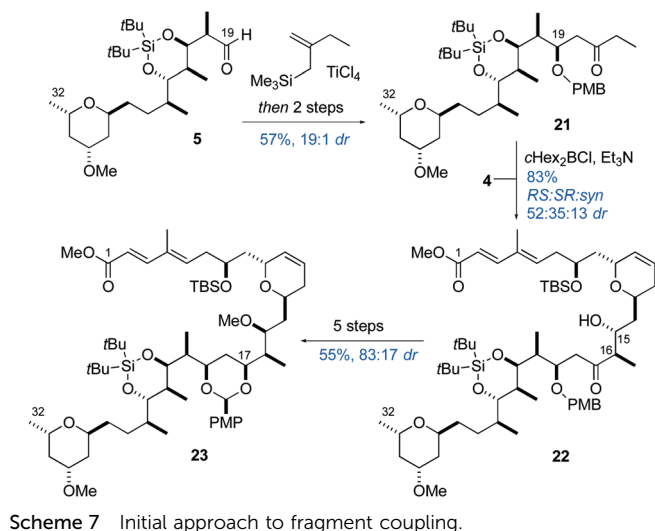
adduct **13**, as predicted by the Evans polar model.<sup>18</sup> Subsequent manipulation, which included an HWE olefination, finally gave C1–C15 aldehyde **4**.

Construction of the corresponding C19–C32 aldehyde **5** (Scheme 6)<sup>19</sup> began with a Sharpless asymmetric epoxidation with kinetic resolution of racemic allylic alcohol **14** to give, after hydroxyl-directed reduction, 1,3-diol **15**. Ozonolysis of the alkene, followed by cyclisation and methylation, gave acetal **16**. This underwent a TMSOTf-catalysed allylation with allyltrimethylsilane to set the C27 stereocentre, followed by elaboration into aldehyde **17**. A *c*Hex<sub>2</sub>BCl-mediated aldol reaction, between Roche ester-derived ethyl ketone **18** and aldehyde **17**, afforded *anti* adduct **19**. This underwent an Evans–Saksena 1,3-*anti* reduction and silylation to produce alkene **20**. Subsequent hydroboration with thexylborane, followed by a site-specific



Scheme 6 Synthesis of C19–C32 aldehyde **5**.





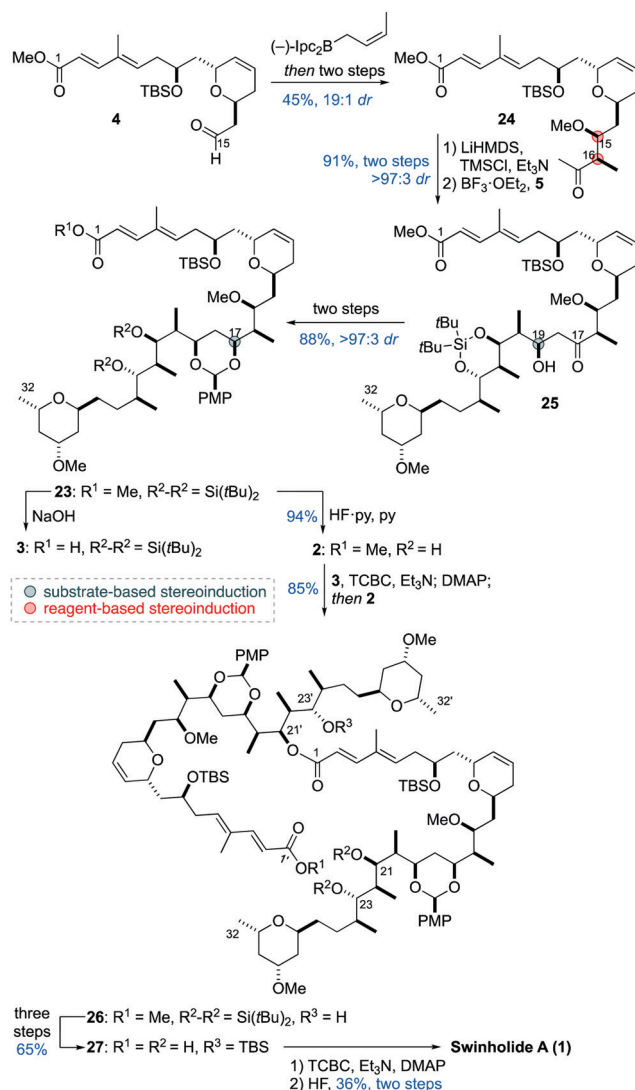
deoxygenation sequence, then afforded the fully elaborated C19–C32 aldehyde **5**, with efficient substrate-controlled installation of the five contiguous stereocentres.

Moving forward, investigation of the  $c\text{Hex}_2\text{BCl}$ -mediated aldol coupling between C16–C32 ethyl ketone **21** (Scheme 7) derived from aldehyde **5** with C1–C15 aldehyde **4** revealed only a moderate level of diastereoselectivity for *anti* adduct **22**.<sup>20</sup> Although this product could be inverted at C15 and elaborated into monomeric unit **23**,<sup>21</sup> this less than satisfactory result detracted from the otherwise excellent level of stereocontrol achieved. Fortunately, an alternative fragment coupling proved superior, where C1–C15 aldehyde **4** was first submitted to a Brown crotylation, followed by elaboration into methyl ketone **24** (Scheme 8). The complex aldol coupling between the silyl enol ether derivative of **24** and **5** was then best performed under Mukaiyama conditions, mediated by  $\text{BF}_3 \cdot \text{OEt}_2$ . This efficiently gave adduct **25**, as predicted by the Felkin–Anh model. Finally, a 1,3-*syn* reduction of **25** installed the C17 stereocentre, followed by conversion into PMP acetal **23**.

At this advanced stage of the campaign, an adventurous site-selective dimerisation of monomeric unit **23** was required to construct the signature macrodiolide of swinholid A. In practice, **23** was differentially desilylated under fluororous conditions to give diol **2**, while ester hydrolysis gave acid **3**. Initial studies revealed that site-selectivity was sensitive to the esterification conditions employed.<sup>22</sup> Notably, Yamaguchi conditions resulted in preferential esterification at the desired C21 alcohol. Thus, diol **2** and acid **3** were first selectively coupled to give C21' ester **26**. Gratifyingly, after its controlled conversion into *seco* acid **27**, a site-selective Yamaguchi macrolactonisation, at the desired C21 alcohol, served to assemble the desired 44-membered macrodiolide core. Finally, an uneventful global deprotection step enabled the first total synthesis of swinholid A (**1**) in 25 steps longest linear sequence (LLS) and 0.4% yield.<sup>23,24</sup>

### 3.2 Spongistatin 1/altohyrtin A

The spongistatins (also known as the altohyrtins) are a family of extremely potent antimitotic macrolides. In 1993, members of

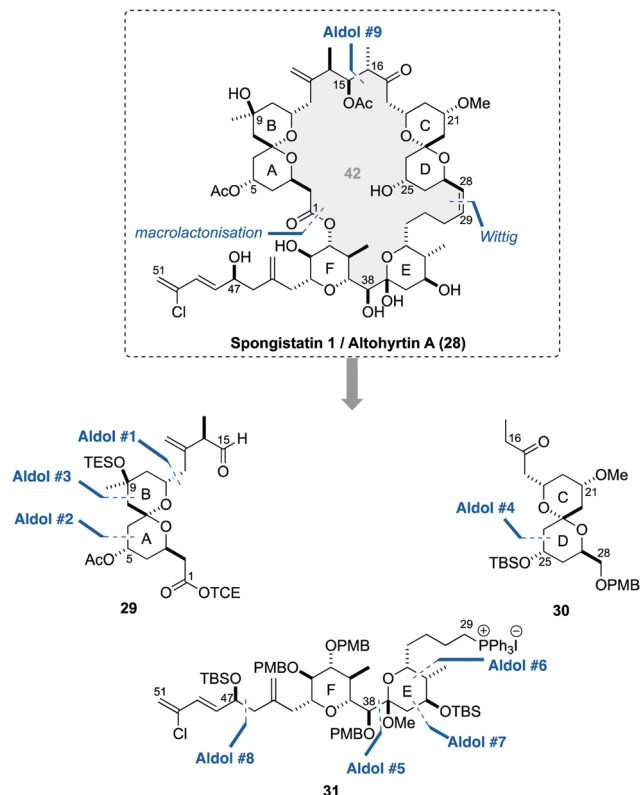


**Scheme 8** Alternative coupling sequence and completion of the total synthesis of swinholid A (**1**).

this family were independently reported to be isolated from marine sponges by the groups of Pettit,<sup>25</sup> Kobayashi/Kitagawa<sup>26</sup> and Fusetani.<sup>27</sup> While there was initially variation in the configurational assignments, the first total synthesis by the Evans group,<sup>28</sup> followed by that of the Kishi group,<sup>29</sup> confirmed the assignment of Kobayashi/Kitagawa and established that altohyrtins A and C were identical to spongistatins 1 and 2, respectively. Structurally, spongistatin 1 (**28**, Scheme 9) features an elaborate 51-carbon backbone, bearing 24 stereocentres, and incorporates a highly substituted 42-membered macrolactone with a chlorotriene side chain. The macrolactone core itself encompasses the AB spiroacetal, the CD spiroacetal and the bis-tetrahydropyran EF rings.

This macrolide chemotype is amongst the most potent compounds to be tested in the NCI panel of human carcinoma cell lines, with exemplary picomolar cytotoxicity. Furthermore, *in vivo* human carcinoma xenograft studies showed curative responses for ovarian tumours and melanoma at extremely low





Scheme 9 Structure and retrosynthetic analysis of spongistatin 1/altohyrtin A (28), highlighting the nine aldol disconnections.

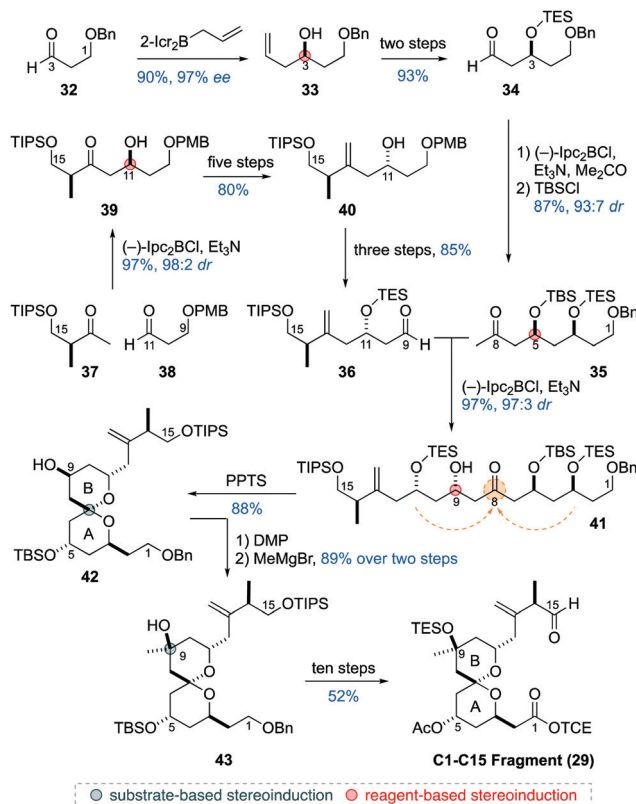
dosage levels.<sup>30</sup> Recent X-ray crystallographic studies of the spongistatin 1/tubulin complex revealed that the spongistatins bind to the maytansine domain of tubulin,<sup>31</sup> which prevents microtubule assembly, thereby inhibiting mitosis.<sup>32</sup> Despite such promising preclinical results, their meagre and unsustainable natural supply stalled further development. Augmented by its impressive bioactivity and the extreme paucity in natural supply, the extraordinary molecular architecture of spongistatin 1 renders it a compelling synthetic target.<sup>33</sup> Falling under its spell, we viewed it as the definitive complex macrolide to showcase the aldol methodology developed in the group.<sup>34</sup> We aimed to devise a flexible and convergent synthesis that was efficient enough to deliver useful quantities and permit further biological studies.

From the outset of this ambitious campaign, the key concern was how to achieve both high levels of stereocontrol and chemoselectivity, in managing the array of potentially reactive functionalities. In particular, the correct choice of protecting groups and ordering of functional group transformations would be vital in engineering the construction and coupling of the highly oxygenated intermediates. After several iterations, our strategy evolved to target three key fragments – C1–C15 AB spiroacetal 29, C16–C28 CD spiroacetal 30 and C29–C51 EF bis-tetrahydropyran 31. This plan entailed a late-stage macrolactonisation, a Wittig reaction to install the C28–C29 olefin, and an aldol coupling reaction to forge the C15–C16 bond and associated stereocentres. We envisaged that an expedient synthesis could be

enabled through a carefully choreographed sequence of nine boron-mediated aldol reactions. Consequently, spongistatin 1 stands out as a second career highlight.

Assembly of C1–C15 AB spiroacetal 29 (Scheme 10) included three boron-mediated aldol reactions, in which reagent control with (–)-Ipc<sub>2</sub>BCl was used to reinforce any substrate-based stereoinduction.<sup>35</sup> To begin, a modified Brown allylation of aldehyde 32, mediated by (+)-2-carene derived ligands, gave homoallylic alcohol 33. After conversion into aldehyde 34, an aldol reaction with acetone, followed by silylation, generated ketone 35. Synthesis of the corresponding C9–C15 partner 36 began with an aldol reaction between ketone 37 and aldehyde 38 to give 1,4-*syn* adduct 39. Although this led to the epimeric configuration at C11, the excellent yield and selectivity rendered a downstream invertive process the preferred means to obtain the desired C11 stereocentre. This approach entailed protecting group manipulation and a Takai methylenation, before a Mitsunobu reaction gave inverted alcohol 40, which was converted into aldehyde 36.

A complex boron-mediated aldol coupling reaction was now conducted between chiral methyl ketone 35 and chiral aldehyde 36. Employing (–)-Ipc<sub>2</sub>BCl/Et<sub>3</sub>N, this gave exclusively 1,5-*anti* adduct 41. The excellent stereocontrol is attributed to the synergistic combination of the 1,3-*syn* preference of 36, the 1,5-*anti* preference<sup>36</sup> of 35 and the influence of the chiral reagent.<sup>7</sup> Next, selective desilylation of ketone 41 served to construct the *doubly* anomERICALLY-stabilised, axial-axial, AB



Scheme 10 Synthesis of C1–C15 aldehyde 29.



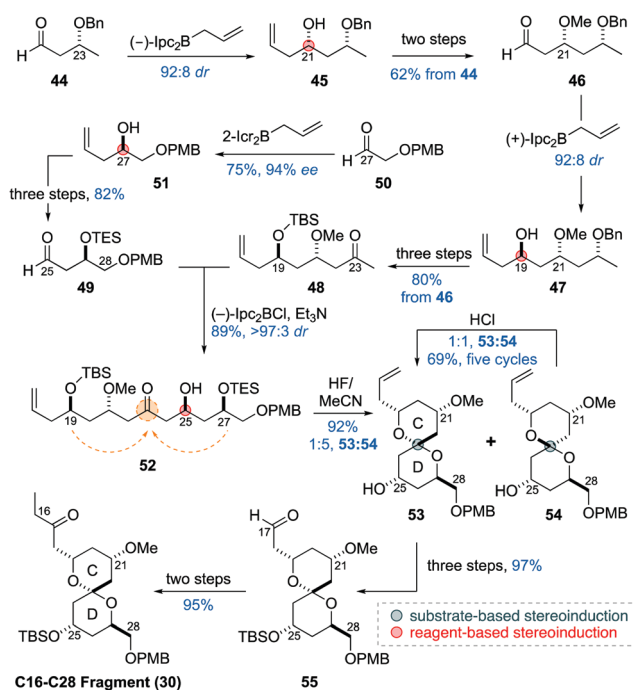
spiroacetal **42**. Oxidation, followed by an axial Grignard addition, then gave alcohol **43**. Finally, a sequence of fine-tuning of protecting groups and oxidation state adjustment afforded C1–C15 aldehyde **29**.

The synthesis of the corresponding C16–C28 fragment **30** proved to be a hurdle, owing to the *singly* anomerically-stabilised, axial-equatorial, CD spiroacetal.<sup>37</sup> An initially explored kinetic approach proved disappointing, as only a slight preference for the desired spiroacetal configuration was observed. Ultimately, an equilibration approach (Scheme 11) became the preferred route, with the stereocentres introduced by three reagent-controlled allylations and an aldol reaction. This commenced with a Brown allylation of aldehyde **44** to give alcohol **45**. Following methylation and ozonolysis, a further allylation of aldehyde **46** gave alcohol **47**. This was then elaborated into methyl ketone **48**, in readiness for a downstream aldol coupling. Synthesis of its aldehyde partner **49** employed a modified Brown allylation, from aldehyde **50**, to generate homoallylic alcohol **51**. This was followed by silylation and oxidative alkene cleavage to give aldehyde **49**.

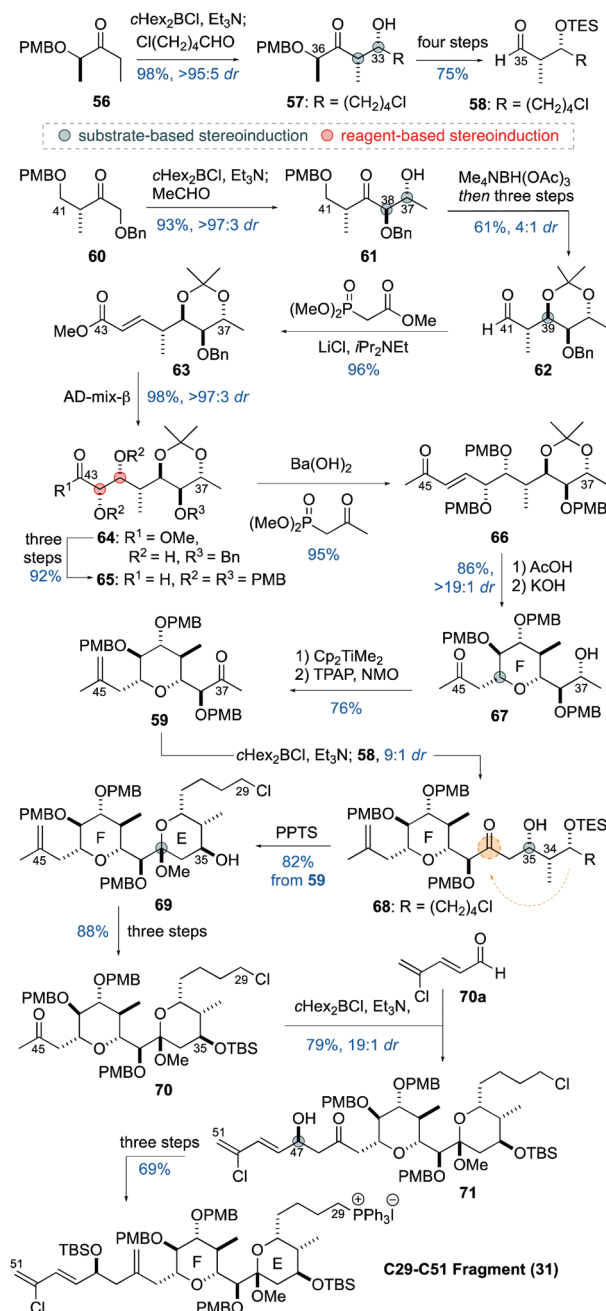
A complex aldol coupling between chiral methyl ketone **48** and chiral aldehyde **49** was then performed using (–)-Ipc<sub>2</sub>BCl/Et<sub>3</sub>N, proceeding with triple asymmetric induction to provide solely adduct **52**. From here, desilylation and concomitant spiroacetalisation, followed by acetal equilibration, under acidic conditions, gave an equimolar mixture of **53** to **54**. At this juncture, chromatographic separation, followed by re-equilibration of the undesired spiroacetal **54**, allowed gram quantities of CD spiroacetal **53** to be accumulated. For the remainder of the campaign, there was a risk that unanticipated re-equilibration of the C23 configuration might occur. Hence, any acidic conditions needed to be avoided. Following conversion into

aldehyde **55**, a Grignard addition and oxidation then produced the complete C16–C28 ketone **30**.

The synthesis of the C29–C51 EF bis-tetrahydropyran motif of spongistatin constituted a logistical challenge. This was both due to the range of potentially reactive functionalities present and the increased stereochemical complexity relative to the other fragments.<sup>34,38</sup> Given that the planned coupling between the northern and southern hemispheres involved a Wittig reaction with an advanced C1–C28 aldehyde, an efficient construction of phosphonium salt **31** was sought (Scheme 12). The boron-mediated aldol reactions used to assemble this fragment enabled the expedient formation of four key carbon–carbon



Scheme 11 Synthesis of C16–C28 ketone **30**.



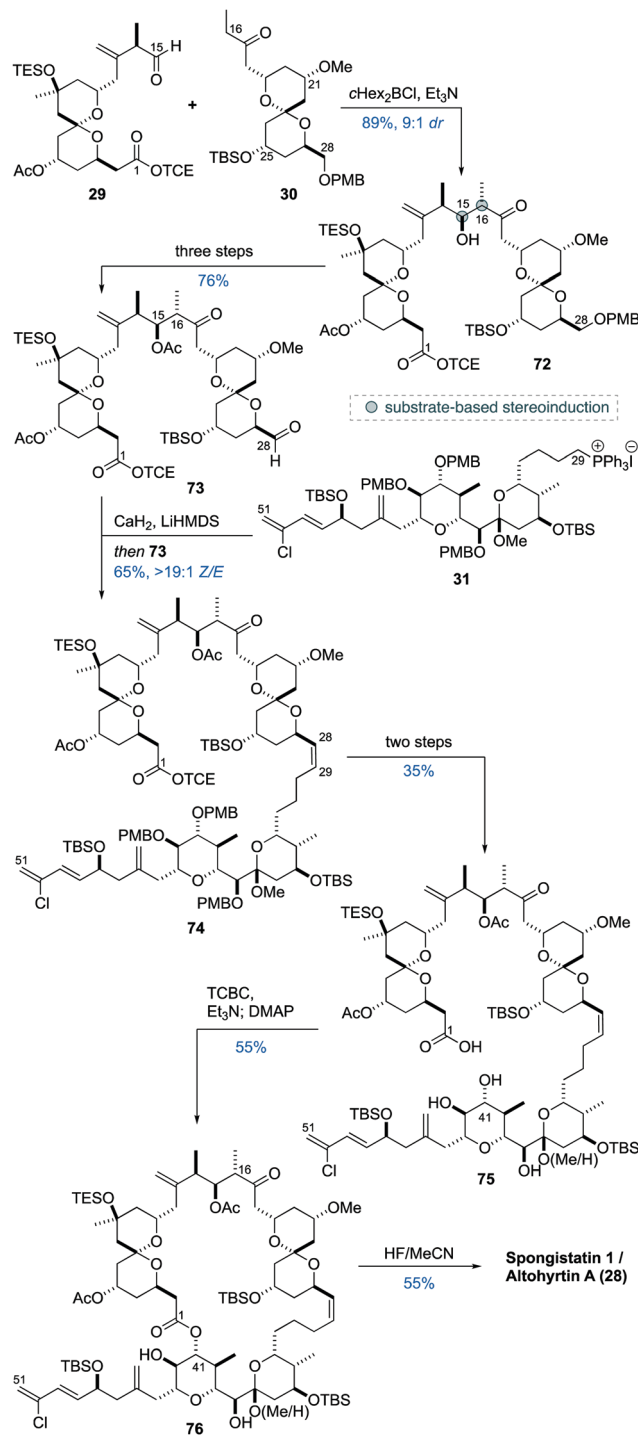
Scheme 12 Synthesis of C29–C51 phosphonium salt **31**.

bonds and six associated stereocentres. Thus, synthesis of the E ring precursor began with a *c*Hex<sub>2</sub>BCl-mediated aldol reaction between lactate-derived ketone **56** and 5-chloropentanal to give *syn* adduct **57**. This was then elaborated into aldehyde **58**, in anticipation of a further aldol coupling reaction.

Synthesis of F ring coupling partner **59** commenced with a substrate-controlled *c*Hex<sub>2</sub>BCl-mediated aldol reaction between Roche ester-derived ketone **60** and acetaldehyde to give *anti* adduct **61**. An Evans–Saksena reduction then gave the corresponding 1,3-*anti* diol, which was transformed into aldehyde **62**. Following HWE olefination to give enoate **63**, a reagent-controlled dihydroxylation under Sharpless conditions<sup>39</sup> delivered diol **64**. Further protecting group and oxidation state manipulation gave aldehyde **65**, enabling a second HWE olefination to give enone **66**.<sup>40</sup> At this point, acid-mediated acetonide cleavage induced a hetero-Michael addition to generate a mixture of tetrahydropyrans. These were equilibrated under basic conditions, to produce the required all-equatorial F ring **67**.

Once the chlorotriene moiety was installed, it was desirable to minimise the number of transformations undertaken in the presence of this delicate moiety. Thus, elaboration at C36 of **59** and coupling with aldehyde **58**, followed by introduction of the full side chain, was planned. To this end, the C45 ketone was transiently masked through methylenation, followed by oxidation at C37 to afford methyl ketone **59**. The aldol construction of the C35–C36 bond proved to be challenging, attributed to steric congestion inhibiting the enolisation of **59**. This necessitated the use of *c*Hex<sub>2</sub>BBr as a more reactive Lewis acid. After coupling with aldehyde **58**, this afforded adduct **68** as predicted by the Felkin–Anh model. Subsequent silylation and acid-catalysed cyclisation then produced E-ring acetal **69**, which was elaborated into ketone **70**. Next, installation of the chlorotriene moiety in **71** was secured by a substrate-controlled *c*Hex<sub>2</sub>BCl-mediated aldol reaction, between ketone **70** and aldehyde **70a**. Unexpectedly, the 1,5-*anti* stereoinduction<sup>36</sup> normally seen in related aldol reactions of simpler β-alkoxy methyl ketones was reversed, ascribed to the opposing influence of the proximate F ring motif.<sup>41</sup> Fortunately, this serendipitous outcome instead gave the required 1,5-*syn* adduct **71**, which was converted into phosphonium salt **31**. Notably, the primary chloride survived throughout, prior to its substitution with triphenylphosphine, without encountering any chemoselectivity issues.

With all three major fragments secured, their controlled coupling and the pivotal macrolactonisation step were pursued.<sup>34,41</sup> The substrate-controlled fragment coupling of C1–C15 aldehyde **29** and C16–C28 ethyl ketone **30** is one of the most complex examples of a boron-mediated aldol reaction (Scheme 13).<sup>42</sup> Use of *c*Hex<sub>2</sub>BCl/Et<sub>3</sub>N to generate the *E*-enolate from **30** and addition to **29** proceeded smoothly to give *anti* adduct **72**, installing the C15 and C16 stereocentres with high fidelity. Following conversion into aldehyde **73**, the challenging Wittig reaction, with phosphonium salt **31**, proved to be an additional hurdle to overcome. After extensive experimentation, a rigorously de-oxygenated solvent mixture of THF/HMPA was found to be optimum, along with treatment of phosphonium salt **31** with CaH<sub>2</sub>, prior to deprotonation (LiHMDS) and addition of



Scheme 13 Completion of the total synthesis of spongistatin 1/altohyrtin A (**28**).

aldehyde **73**. This protocol enabled the Wittig coupling to reproducibly proceed in good yield, to give solely *Z*-alkene **74**. From here, a sequence of PMB ether and TCE ester cleavage produced *seco* acid **75**. Under Yamaguchi conditions, **75** reacted site-selectively, at the C41 alcohol, to give exclusively 42-membered macrolactone **76**. Finally, a global deprotection concluded this eventful synthetic saga and delivered spongistatin 1 (**28**) in 33 steps LLS and 1.6% yield.



The resulting supply of synthesised spongistatin 1 augmented the meagre quantity isolated from > 400 kg of sponge by the Pettit group, enabling the continuation of its biological evaluation, including preliminary SAR studies and mapping of its tubulin binding site.<sup>31</sup> Serendipitously, a side-product with a dehydrated E ring, obtained in the final deprotection step, transpired to be an even more potent cytotoxic agent than the parent natural product.<sup>43</sup>

### 3.3 Spirastrellolide A methyl ester

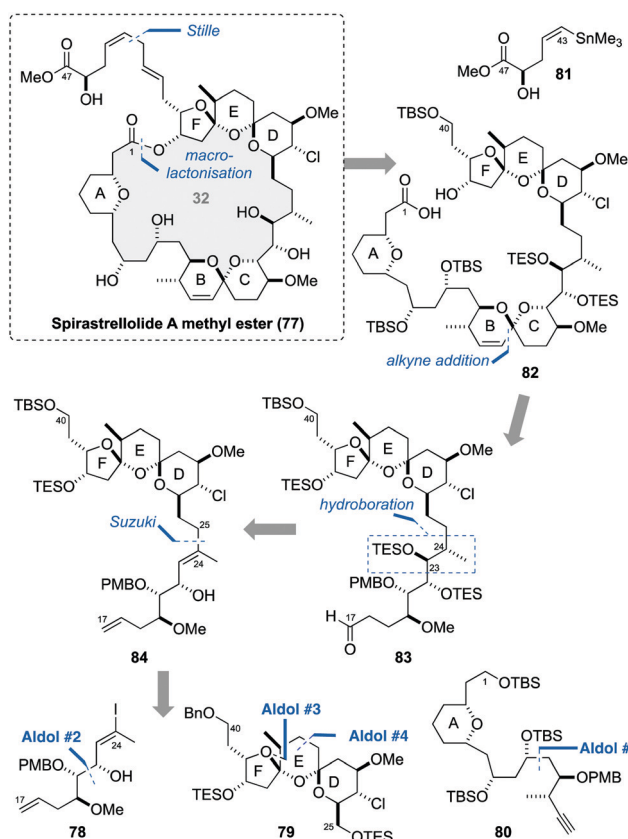
Spirastrellolide A was first reported in 2003 by the Andersen group, following its isolation from the Caribbean sponge *Spirastrella coccinea*.<sup>44</sup> Characterised as its methyl ester 77 (Scheme 14), it showed potent antiproliferative activity against cancer cell lines and acted as a selective inhibitor of Ser/Thr phosphatase 2A.<sup>45</sup> Structurally, it features a 47-carbon skeleton and 21 stereocentres, with a 38-membered macrolide, bearing a skipped diene side chain. The macrocyclic core contains a tetrahydropyran (A ring), a 6,6-spiroacetal (BC rings) and a chlorinated 5,6,6-bis-spiroacetal (DEF rings).

The promising biological properties of spirastrellolide A and its natural scarcity, along with a complex molecular architecture reminiscent of spongistatin and an incomplete stereochemical assignment, provided compelling reasons for pursuing its total synthesis.<sup>46–48</sup> As such, spirastrellolide stands out as a third career highlight. These studies evolved alongside the ongoing

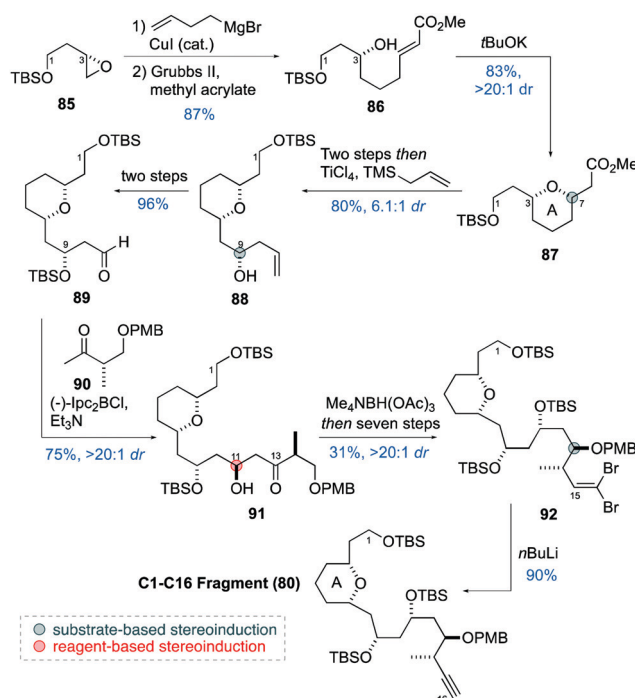
structural elucidation of this intriguing marine macrolide by the Andersen group.

The stereochemical ambiguities demanded a flexible modular approach, whereby each of the three fragments **78**, **79** and **80** were to be constructed with versatile coupling handles. Installation of the side chain, by attachment of stannane **81** to a preformed macrocycle derived from *seco* acid **82**, was planned. Two key disconnections were made: at C16–C17 to disassemble the BC spiroacetal, to reveal fragments **80** and **83**; and at C24–C25 in **84** to reveal fragments **78** and **79**.<sup>49</sup> Four aldol bond constructions were identified for access to these fragments.

Synthesis of C1–C16 alkyne **80** (Scheme 15)<sup>50</sup> commenced with a Grignard addition into epoxide **85**, followed by olefin cross-metathesis with methyl acrylate, to give enoate **86**. This enabled a hetero-Michael addition to install the *cis*-tetrahydropyran A ring in **87**. After conversion into the corresponding C9 aldehyde, a chelation-controlled Hosomi–Sakurai allylation, mediated by TiCl<sub>4</sub>, gave alcohol **88**. The derived C11 aldehyde **89** then underwent a reagent-controlled aldol reaction, mediated by (–)-Ipc<sub>2</sub>BCl, with methyl ketone **90** to afford 1,4-*syn* adduct **91**. Following an Evans–Saksena reduction, this was manipulated to give vinyl dibromide **92**. Finally, treatment with *n*BuLi allowed controlled conversion into alkyne **80**, affording a robust route adaptable to a gram-scale synthesis. The route to C17–C24 vinyl iodide **78** commenced with hydrotitanation/iodination of alkyne **93** (Scheme 16).<sup>51</sup> The derived aldehyde **94** then underwent an Evans glycolate aldol addition with **95** to produce *syn* adduct **96**. Transamination, followed by silylation and allylation, gave ketone **97**. A chelation-controlled ketone reduction, mediated by Zn(BH<sub>4</sub>)<sub>2</sub>, set the final C20 stereocentre. Further adjustment then delivered C17–C24 vinyl iodide **78**.

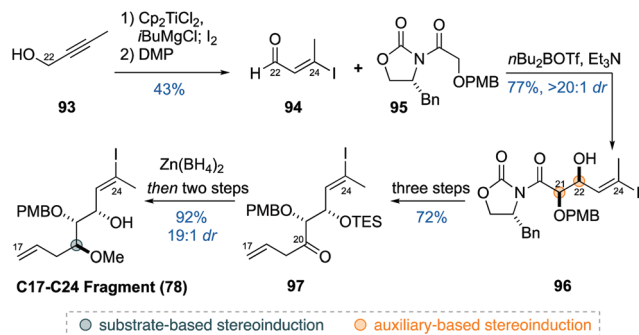


Scheme 14 Structure and retrosynthetic analysis of spirastrellolide A methyl ester (**77**), highlighting the four aldol disconnections.



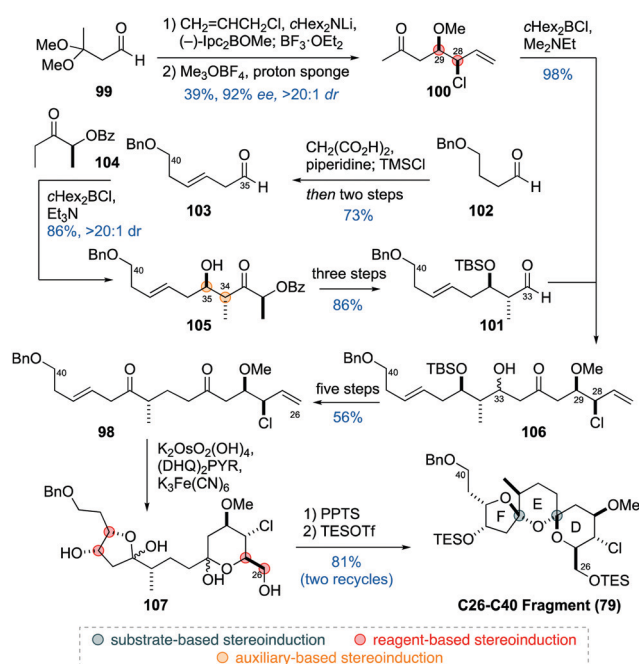
Scheme 15 Synthesis of C1–C16 alkyne **80**.



Scheme 16 Synthesis of C17–C24 vinyl iodide **78**.

The synthesis of the DEF-containing bis-spiroacetal fragment **79** (Scheme 17) underwent continuous refinement during the course of the campaign.<sup>52–54</sup> Recognising that the bis-spiroacetal is doubly stabilised by the anomeric effect suggested cyclisation from a suitable linear precursor under acidic conditions. To streamline the route, the installation of both sets of diols in a single step was proposed, using a Sharpless asymmetric dihydroxylation<sup>39</sup> on diene **98**. Ultimately, this led to the pursuit of an adventurous strategy, centred on the implementation of a double dihydroxylation/spiroacetalisation cascade.<sup>55</sup>

Synthesis of fragment **79** commenced *via* an Oehlschlager–Brown chloroallylation<sup>56</sup> of aldehyde **99**, followed by acetal cleavage and methyl ether formation, to give *syn* adduct **100**. The corresponding C33–C40 aldehyde **101** was prepared from aldehyde **102**, utilising an Knoevenagel-type condensation with malonic acid. A *c*Hex<sub>2</sub>BCl-mediated aldol reaction between aldehyde **103** and ethyl ketone (*S*)-**104** then delivered *anti* adduct **105**, which was taken on to C33 aldehyde **101**. At this

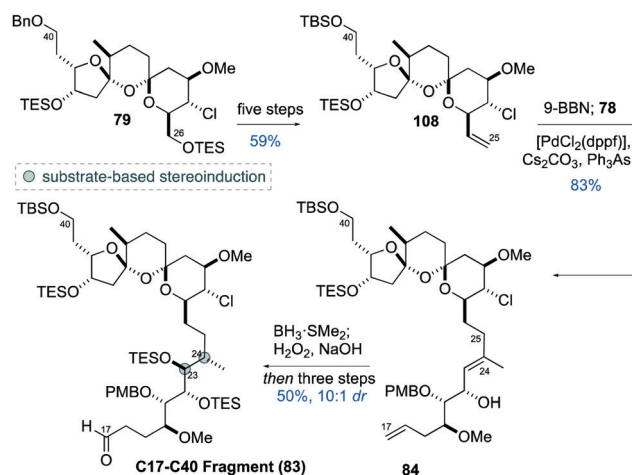
Scheme 17 Synthesis of C26–C40 fragment **79**.

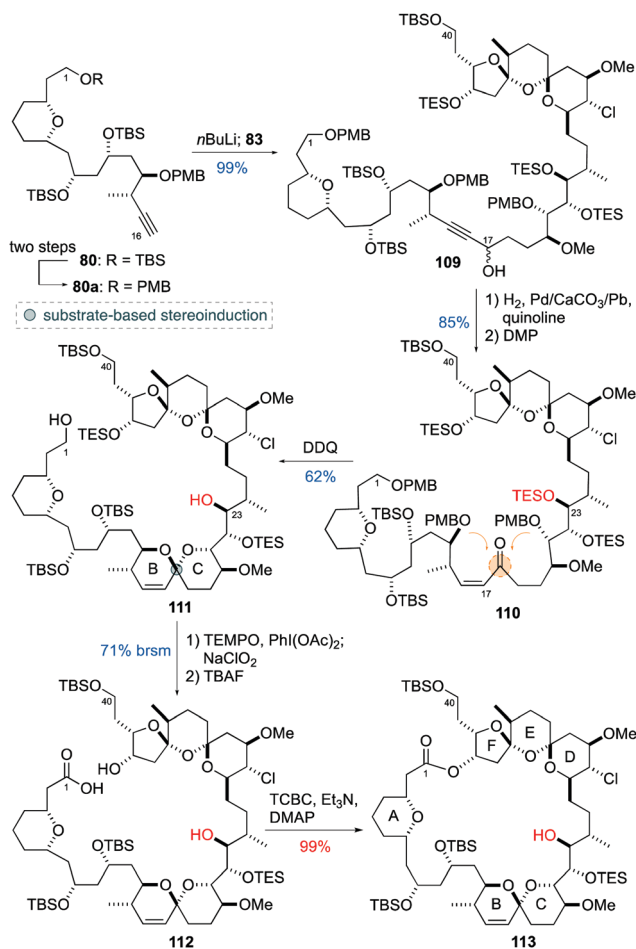
point, fragment union, through an aldol coupling of methyl ketone **100** and aldehyde **101**, gave C26–C40 adduct **106**. This was elaborated into the required diene **98** for the projected double dihydroxylation/spiroacetalisation cascade. This reaction initially produced a complex mixture of hemiacetals **107**. Gratifyingly, when exposed to mild acidic conditions, cyclisation occurred to deliver the desired DEF-containing bis-spiroacetal, which was then silylated to give **79**. Notably, this expedient cascade route proved to be readily scalable, delivering gram quantities of **79**.

The planned fragment union was now executed *via* a Suzuki coupling (Scheme 18). From **79**, conversion into alkene **108** enabled hydroboration and Pd-catalysed sp<sup>2</sup>–sp<sup>3</sup> cross-coupling with vinyl iodide **78** to give diene **84**. Next, the crucial double hydroboration using BH<sub>3</sub>·SMe<sub>2</sub> served to install the primary C17 alcohol, as well as correctly configuring the C23 and C24 stereocentres. This was followed by its advancement to C17–C40 aldehyde **83**.

With the C17–C40 aldehyde secured, coupling with the C1–C16 fragment **80a** and spiroacetalisation to complete the cyclic ether skeleton was addressed (Scheme 19). Lithiation of alkyne **80a** and addition to aldehyde **83** proceeded smoothly to deliver C1–C40 alcohol **109**. A Lindlar reduction and oxidation gave *Z*-enone **110**.

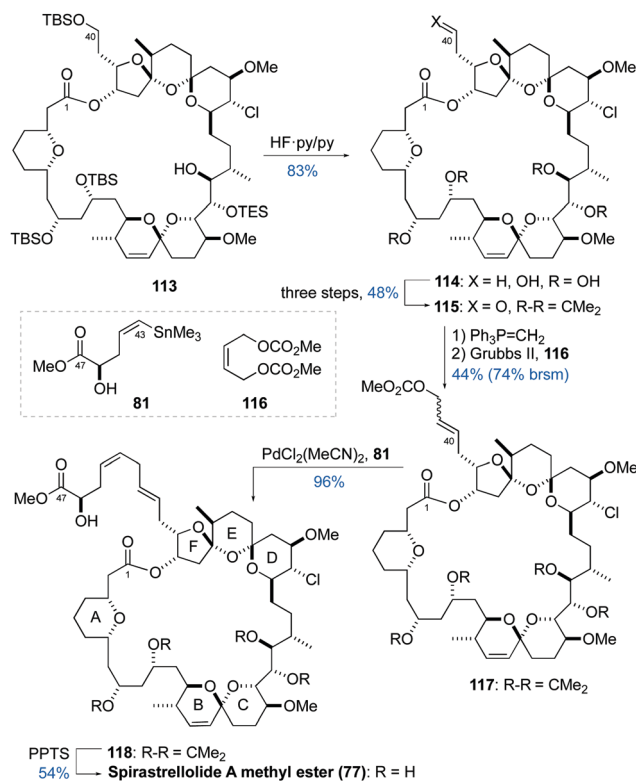
On exposure to DDQ, this underwent global PMB ether cleavage at C1, C13 and C21, enabling facile cyclisation to afford spiroacetal **111**. These mildly acidic reaction conditions also caused unexpected desilylation at C23 to reveal the highlighted secondary alcohol. Considered an annoyance and inconsequential at the time, this unintended deprotection turned out to be profoundly important. From **111**, oxidation, followed by selective C37 desilylation, provided *seco* acid **112**. Under Yamaguchi conditions, this delivered 38-membered macrolactone **113**, in essentially quantitative yield. In our experience, this welcome result stands as a record yield for a macrolactonisation performed on a complex *seco* acid. The ease and striking efficiency of this crucial macrocyclisation reaction is attributed to a favourable conformational pre-organisation in **112**.

Scheme 18 Synthesis of C17–C40 aldehyde **83**.

Scheme 19 Synthesis of macrolactone **113**.

From macrocycle **113**, side chain attachment appeared to be the final hurdle to surmount. However, there proved to be an unanticipated sting in the tail! Frustratingly, selective desilylation at C40 resisted all attempts, necessitating a switch in protecting groups. Nevertheless, this led to a lucky break. Global desilylation of **113** afforded highly crystalline pentaol **114**, which was submitted to single-crystal X-ray crystallographic analysis (Scheme 20). Gratifyingly, this confirmed the configuration of all the stereocentres that had been installed, as well as revealing the network of H-bond interactions within the macrocyclic core.<sup>57</sup> From here, the diols were converted into the corresponding acetonides, permitting controlled manipulation at C40 for side chain installation. Disappointingly, a number of approaches proved to be unsuccessful, which was attributable to the steric encumbrance of the macrocycle. Nonetheless, it was found that Wittig methylenation, followed by olefin cross-metathesis (Grubbs II) with alkene **116**, gave allylic carbonate **117**. This enabled a  $\pi$ -allyl Stille coupling with stannane **81** to deliver the full C1–C47 skeleton in **118**. Finally, a global deprotection completed the first total synthesis of spirastrellolide A methyl ester (**77**),<sup>46</sup> and unambiguously confirmed the full 3D molecular structure for what started out as a dynamic target.

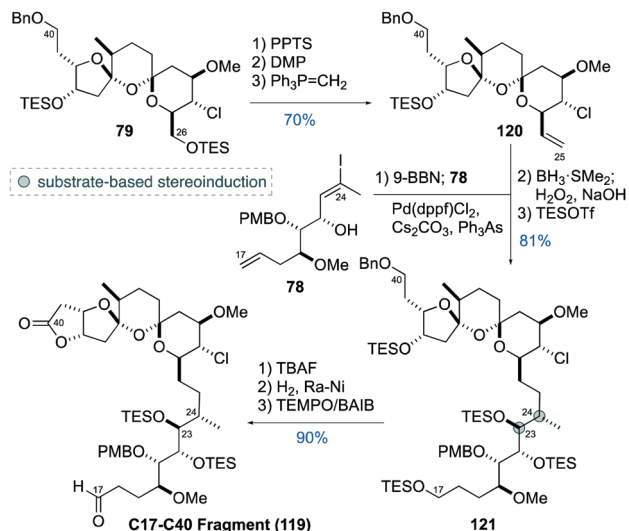
Following on from this success, we pursued a second-generation synthesis, with a focus on constructing a now fully defined target by

Scheme 20 Completion of the total synthesis of spirastrellolide A methyl ester (**77**).

a more direct route. We aimed to remove redundancies, such as protecting group and oxidation level manipulations, and reduce the overall step count.<sup>47</sup> A major economy was that this was to be pursued by a single student. In addition, we now planned to complete the entire carbon skeleton in the *seco* acid prior to macrolactonisation, circumventing the difficulties experienced with late-stage side chain attachment to the preformed macrocycle. The key fragments from the first-generation synthesis, vinyl iodide **78**, DEF rings **79** and alkyne **80** could again be used in this more streamlined plan.

Formation of C17–C40 aldehyde **119** (Scheme 21) commenced with selective C26 desilylation of **79**, oxidation and Wittig methylenation to give alkene **120**. Hydroboration of **120**, Suzuki coupling with vinyl iodide **78** and double hydroboration proceeded to give C17–C40 fragment **121**. At this point, selective cleavage of the C17 and C37 TES ethers, and debenzoylation gave the corresponding triol. As a finale, a one-pot triple oxidation at C17 and C40 afforded the revised C17–C40 fragment **119**, terminating in a  $\gamma$ -lactone and aldehyde as coupling handles. With all the requisite fragments in hand, the completion of the fully elaborated *seco* acid skeleton was addressed. Frustratingly, initial attempts at reproducing the lithium acetylide addition of alkyne **80** with revised aldehyde **119** failed, due to chemoselectivity issues. Fortunately, this pivotal fragment coupling was efficiently achieved under Nozaki–Hiyama–Kishi conditions with iodoalkyne **122** and aldehyde **119** to form alcohol **123** (Scheme 22). From here, the Lindlar reduction, oxidation and PMB ether cleavage/spiroacetalisation sequence





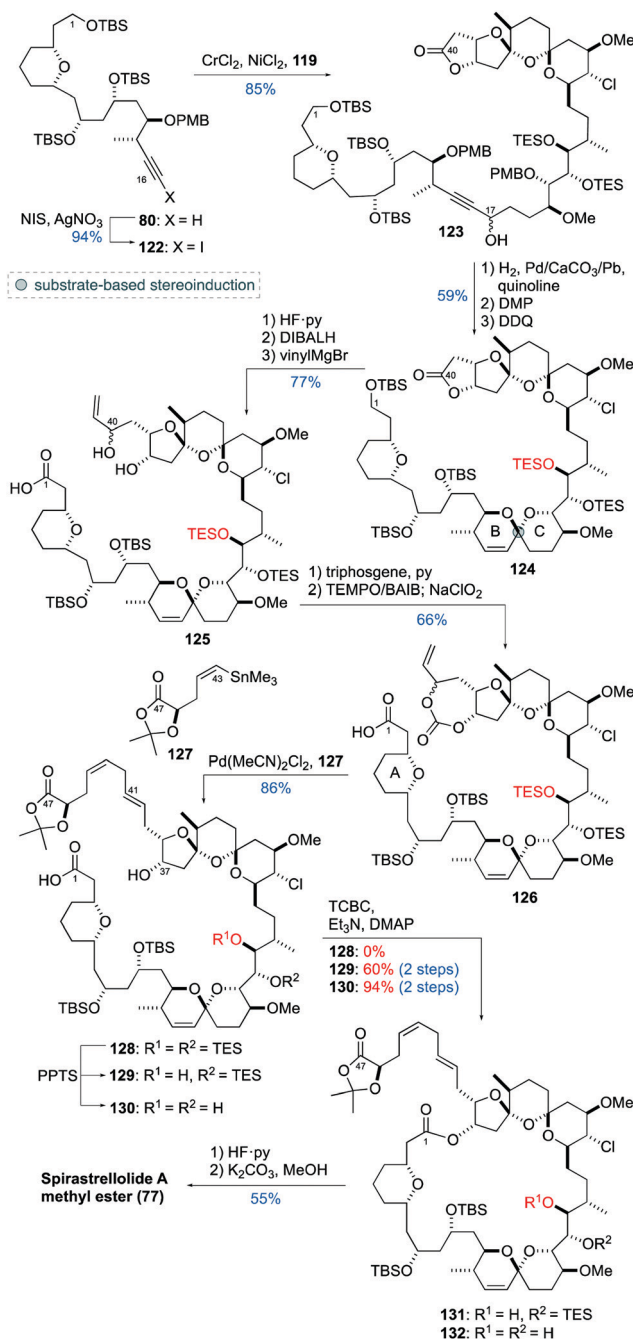
Scheme 21 Synthesis of C17–C40 aldehyde **119** for the second-generation route.

was conducted without incident. This delivered C1–C40 fragment **124**, now retaining the C23 TES ether that had been unexpectedly cleaved in the first-generation synthesis.

At this juncture, the entire spirastrellolide A skeleton now seemed within our grasp. In the event, C1 desilylation, reduction of the  $\gamma$ -lactone and vinyl Grignard addition gave triol **125**. Treatment of **125** with triphosgene, followed by oxidation, then gave acid **126**, bearing a cyclic carbonate motif. Gratifyingly, a  $\pi$ -allyl Stille coupling between acid **126** and stannane **127** smoothly delivered the complete C1–C47 *seco* acid **128**, with concomitant unmasking of the C37 alcohol.

To our dismay, subjecting *seco* acid **128** to Yamaguchi and various other macrolactonisation protocols now failed to produce any desired product! This nightmare scenario prompted a critical examination of the structural differences between the first- and second-generation substrates. After discounting the nature of the side chain being an inhibitory factor, the presence of the C23 TES ether in **128** seemed to be the likely culprit. To probe if this was responsible for this disparate reactivity, *seco* acid **128** was subjected to controlled desilylation to obtain either the C23 alcohol **129** or the C22–C23 diol **130**. Sure enough, submitting **129** and **130** to Yamaguchi conditions led to the immediate return of reactivity, delivering macrolactones **131** and **132**, respectively. With this unforeseen hurdle surmounted and the macrocycle secured, the finishing line was now in sight. From **132**, controlled deprotection delivered spirastrellolide A methyl ester (**77**) in 23 steps LLS and 6% overall yield, representing a marked improvement on the first-generation route.<sup>47</sup>

This demanding project highlights the unseen hand of serendipity in total synthesis endeavours. In hindsight, the successful first-generation route was enabled through the unexpected release of the C23 alcohol during the BC-spiroacetal formation. This unforeseen outcome acts as a reminder of the subtle conformational influence of even distal protecting groups. In this case,



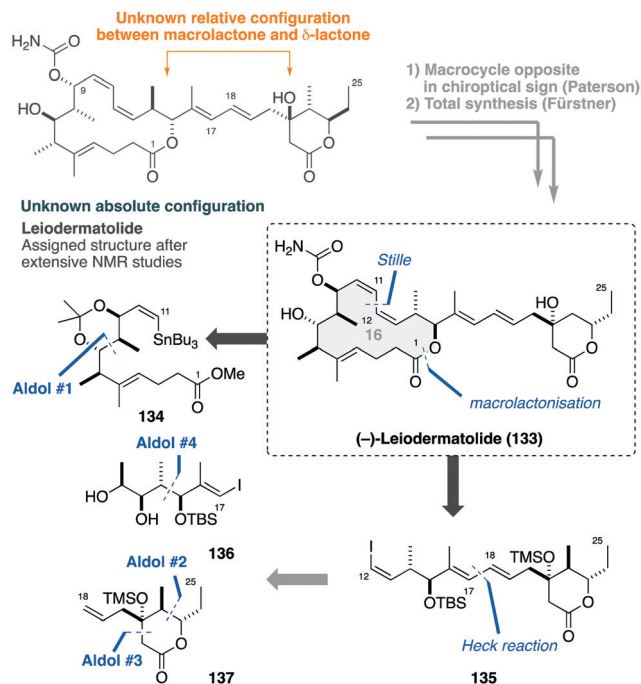
Scheme 22 Completion of the second-generation synthesis of spirastrellolide A (**77**), highlighting the problematic TES ether in the macrolactonisation.

acting to mutate a pre-organised conformation favouring macrocyclisation to one that completely inhibits it.

### 3.4 Leiodermatolide

In 2008, the Wright group disclosed the isolation of leiodermatolide (**133**, Scheme 23) from the lithistid sponge *Leiodermatium* sp., collected off the coast of Florida.<sup>58</sup> This novel macrolide chemotype demonstrated potent antiproliferative and tubulin-binding activity, with a mechanism hypothesised to be orthogonal to existing tubulin-binders. From the outset, we were



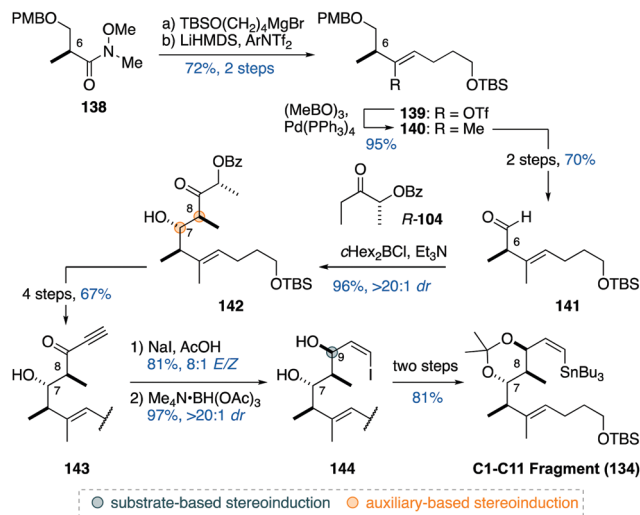


Scheme 23 Overview of the stereochemical assignment of (-)-leidermatolide (133) and its retrosynthetic analysis, highlighting the four aldol disconnections.

intimately involved with its stereochemical elucidation in collaboration with the Wright group, where detailed NMR analysis and computational NMR predictions allowed the determination of the relative configuration of the C1–C15 macrocycle and the C21–C25  $\delta$ -lactone.<sup>59</sup> However, the distal nature of these two stereoclusters precluded a confident assignment of the complete 3D structure, necessitating additional detective work and a focused synthetic campaign. The close involvement from structural characterisation to synthesis places leidermatolide as a fourth career highlight.

In preliminary efforts towards assembling the 16-membered macrolactone core, a specific rotation opposite in sign to the natural product was obtained, tentatively suggesting that we were pursuing the wrong enantiomer.<sup>60,61</sup> Subsequently, the synthesis of two candidate diastereomers of leidermatolide, reported by Fürstner,<sup>62</sup> established the absolute configuration and the relationship between the two stereoclusters as indicated in 133. This prompted a revised strategy, disassembling leidermatolide into two fragments 134 and 135, with a late-stage macrolactonisation.<sup>63</sup> The latter fragment could then be disassembled *via* a Heck reaction to construct the *E,E*-diene, revealing iodide 136 and  $\delta$ -lactone 137. Four key aldol disconnections were identified to install the oxygenation and stereochemistry.

Synthesis of stannane 134 (Scheme 24) commenced with a Grignard addition into Weinreb amide 138, where treatment of the resulting ketone with Comins' reagent, followed by Suzuki cross-coupling of the resulting enol triflate 139, gave *E*-trisubstituted alkene 140. After revealing aldehyde 141, a *c*Hex<sub>2</sub>BCl-mediated aldol reaction, with ethyl ketone (*R*)-104, configured the 7,8-*anti* stereocentres in adduct 142. This was transformed into allknone



Scheme 24 Synthesis of stannane 134.

143, where iodide addition and stereoselective protonation of the intermediate allenol, followed by an Evans–Saksena reduction, configured 1,3-diol 144. From here, acetonide formation and iodine/tin exchange gave stannane 134.

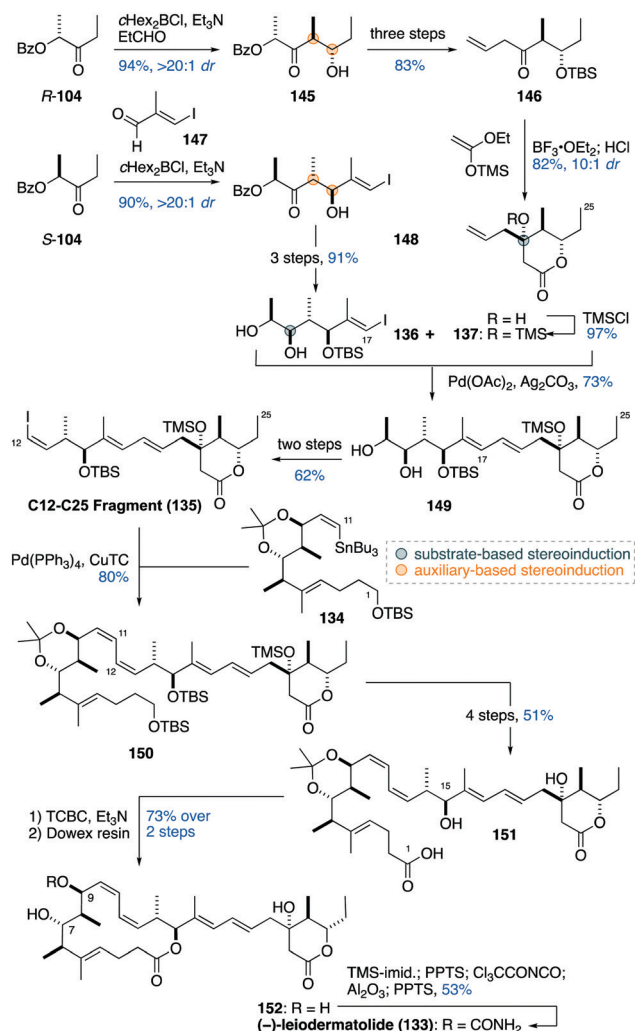
Synthesis of  $\delta$ -lactone 137 (Scheme 25) commenced with a *c*Hex<sub>2</sub>BCl-mediated aldol reaction, between lactate-derived ketone (*R*)-104 and propionaldehyde, to give 145. This was manipulated to afford ketone 146. A sequence of a Mukaiyama aldol reaction, lactonisation and silylation then gave fragment 137. In a similar manner, synthesis of iodide 136 commenced with a lactate aldol reaction, between ketone (*S*)-104 and aldehyde 147 to give adduct 148. This was converted into diol 136, which engaged with alkene 137 in a Heck reaction to generate diene 149. Following transformation into vinyl iodide 135, a pivotal Stille cross-coupling with stannane 134 afforded the full C1–C25 carbon skeleton 150 of leidermatolide.

At this point, the derived *seco* acid 151 was smoothly macrolactonised, under Yamaguchi conditions, and desilylated to give triol 152, in readiness for the endgame. Frustratingly, attempted site-selective carbamoylation of triol 152 favoured the C7 position, contradicting the results from model studies and with other electrophilic reagents, which proved to be an unforeseen roadblock. After extensive experimentation, a carefully choreographed sequence emerged. This involved a transient bis-silylation of C7 and C9, selective desilylation at C9 under acidic conditions, and carbamoylation, followed by global desilylation. Gratifyingly, this afforded (-)-leidermatolide (133) in 23 steps LLS and 3.2% yield, which proved to be identical to an authentic sample in all respects.<sup>59</sup>

### 3.5 Chivosazole F

The chivosazoles are a family of actin-binding terrestrial macrocides, isolated in 1997 by Reichenbach, Höfle and co-workers from *Sorangium cellulosum* myxobacteria.<sup>64</sup> Their full 3D molecular architecture was subsequently determined by Kalesse,<sup>65,66</sup> based on a combination of chemical synthesis, conformational

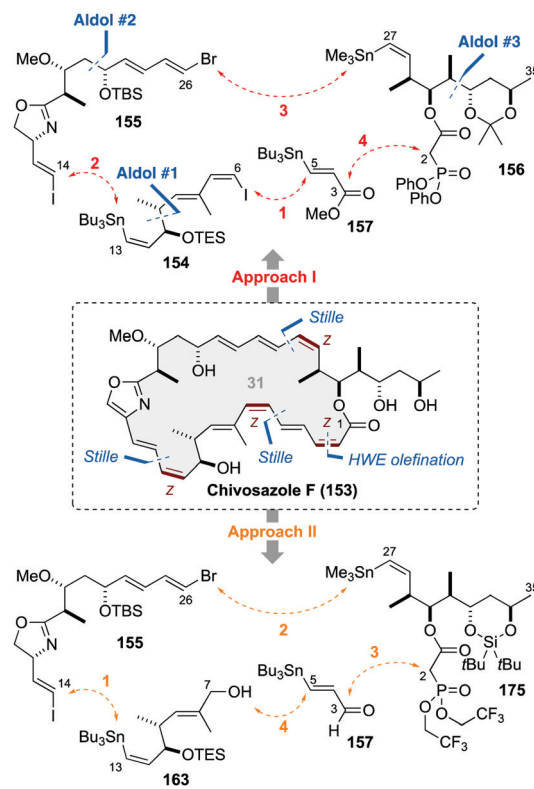


Scheme 25 Completion of the total synthesis of leiodermatolide (**133**).

analysis and genetic analysis. This revealed chivosazole F (**153**, Scheme 26) to be a 31-membered macrolactone, containing an oxazole and three distinct polyene regions, along with 10 stereocentres.

At the outset, the introduction of the stereodefined polyenes with alternating geometry, which were known to readily isomerise, was identified as a key challenge. This challenge did indeed transpire and caused nightmares throughout our synthesis campaign.<sup>67</sup> The frustration associated with this shapeshifting molecule made our eventual success all the sweeter; placing chivosazole F as a fifth career highlight. In an initial approach, three aldol disconnections were proposed in combination with a series of Stille couplings and HWE olefination, to set the geometry of the delicate polyene regions, leading back to four fragments **154–157**.

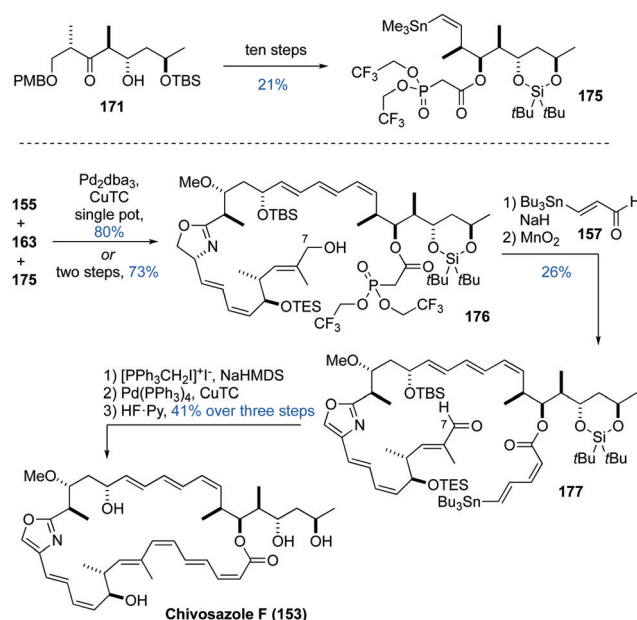
Synthesis of the C6–C13 fragment **154** began from Evans imide **158** (Scheme 27). While it had been initially planned to introduce the required 12Z-alkene *via* a vinylogous aldol reaction with Z-bromoacrolein, this was found to readily isomerise giving an early preview of the unanticipated problems ahead.<sup>68</sup> To circumvent this difficulty, a Kobayashi-type, vinylogous

Scheme 26 Structure and retrosynthetic analysis of chivosazole F (**153**), highlighting the two synthetic approaches based on three aldol disconnections and three Stille couplings.

Mukaiyama aldol reaction,<sup>69</sup> with aldehyde **159**, mediated by  $\text{TiCl}_4$ , afforded the *anti* adduct **160**, which was converted into TES ether **161**. The required 12Z-alkene was now installed *via* a palladium-mediated *trans*-debromination<sup>70</sup> to afford bromide **162**. Following conversion into **163**, installation of the 6Z-vinyl iodide was achieved by a Stork–Zhao olefination<sup>71</sup> to afford C6–C13 fragment **154**. Moving on to the synthesis of C14–C26 fragment **155**, this commenced with an (–)-Ipc<sub>2</sub>BCl-mediated aldol reaction between methyl ketone **164** and bromodienal **165** to afford adduct **166**. Further manipulation gave acid **167**, which was first coupled with amine **168**, before cyclisation to form oxazoline **155**. While the initial plan<sup>72</sup> envisaged conversion into the oxazole at this stage, the oxidation conditions were found to be incompatible with the vinyl iodide, necessitating the postponement of this transformation to after fragment union. Synthesis of the final C27–C35 fragment **156** commenced with a  $\alpha\text{-Hex}_2\text{BCl}$ -mediated aldol reaction, between ketone **169** and aldehyde **170**, to provide *anti* adduct **171**. Following transformation into the corresponding aldehyde **172**, a Stork–Zhao olefination installed the required 27Z-alkene in **173** and further elaboration gave fragment **156**.

For assembling the three alkene fragments **154–156** and acrylate derivative **157**, a suitably choreographed sequence of Stille coupling reactions was sought. This was best accomplished *via* a remarkable one-pot process, involving sequential addition of **154**, **155**, **156** and **157** to a solution of palladium catalyst to progressively assemble **174**. This exquisitely controlled



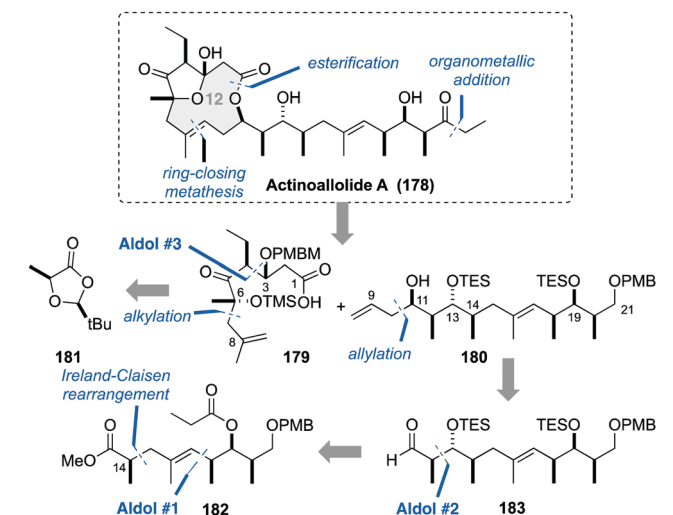


**Scheme 27** Synthesis of key fragments **154**, **155** and **156** and their Stille coupling.

Synthesis of the revised C27–C35 fragment **175** (Scheme 28), incorporating a Still–Gennari-type phosphonate,<sup>73</sup> was achieved from intermediate **171**, setting the stage for exploration of the revised endgame. As before, fragments **155**, **163** and **175** were coupled under mild Stille conditions, either sequentially or in a one-pot operation, providing advanced phosphonate **176**.

### 3.6 Actinoallolide A

Captivated by its intriguing structure and potential as a drug lead in the treatment of neglected tropical diseases, actinoalloyd A was viewed as an important target for realising an efficient total synthesis and exploring its mechanism of action. It was proposed to initially disassemble the lactone linkage and macrocyclic alkene in **178** to reveal C1–C8 alkene **179** and C9–C21 alkene **180**.<sup>75</sup> We envisaged an adventurous ring-closing olefin metathesis (RCM) to install the highlighted trisubstituted

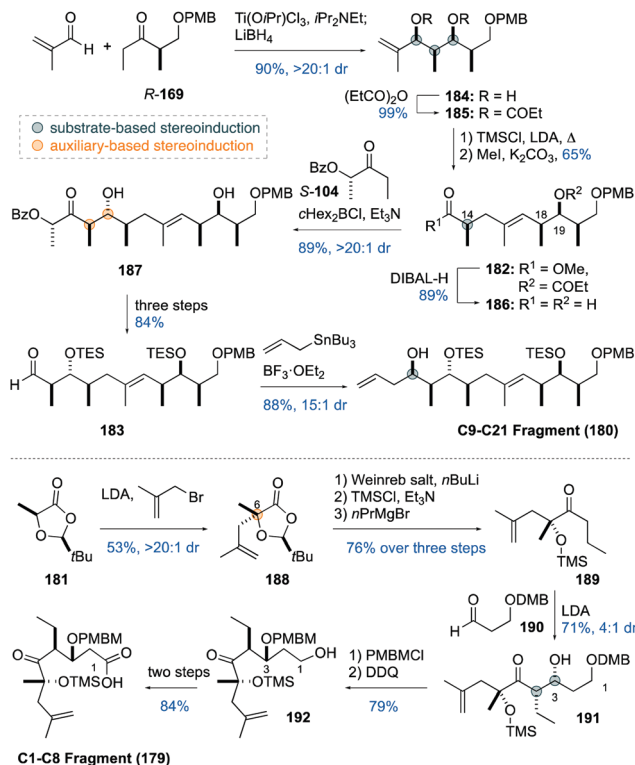


**Scheme 29** Structure and retrosynthetic analysis of actinoallolide A (**178**), highlighting the three aldol disconnections and ring-closing olefin metathesis.

*E*-alkene. However, this “do or die” key step was perceived as a high-risk, high-reward manoeuvre due to the lack of examples in constructing comparable medium-ring systems. The thrill of pursuing such an adventurous RCM approach stands as a sixth career highlight. Fragment **179** was planned to be constructed from dioxolanone **181**<sup>76</sup> and a substrate-controlled aldol reaction. Adapting a strategy from the earlier synthesis of the ebelactones,<sup>77</sup> an Ireland–Claisen rearrangement was selected to configure the distal C14 stereocentre and trisubstituted *E*-alkene in **182**. The C11–C13 region would be introduced, in turn, by a lactate aldol reaction<sup>9</sup> and allylation of aldehyde **183**. Lastly, the C18–C20 stereotriad in **179** would be set by a third aldol reaction.

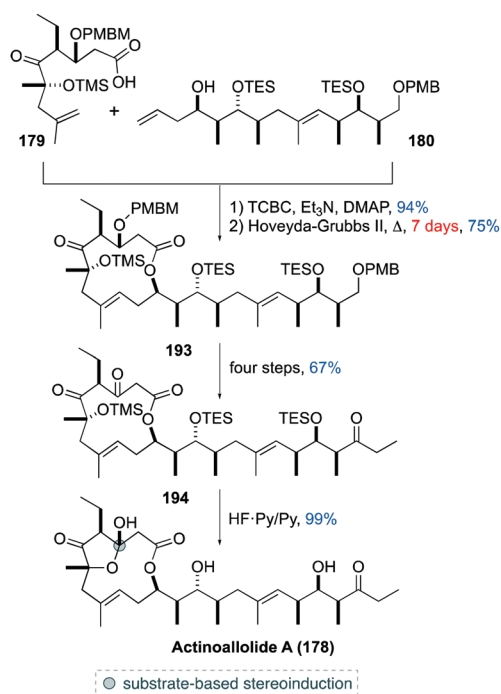
Following this blueprint, the synthesis of side chain fragment **180** (Scheme 30) commenced with a substrate-controlled titanium-mediated aldol reaction,<sup>78,79</sup> between ketone (*R*)-**169** and methacrolein, and *in situ* reduction to provide diol **184**. Esterification afforded **185**, which underwent an Ireland–Claisen rearrangement to efficiently install the desired 1,5-*syn* relationship, between C14 and C18, in *E*-alkene **182**. Reduction of **182** then gave aldehyde **186**, in readiness for a *c*Hex<sub>2</sub>BCl-mediated aldol reaction with ketone (*S*)-**104**. Here  $\pi$ -facial control from the enolate component overrides any inherent bias of the aldehyde to form the desired *anti* adduct **187**. After conversion into aldehyde **183**, Lewis acid-mediated allylation under Hosomi–Sakurai conditions, exploiting the Felkin–Anh model reinforced by the Evans polar model, served to complete the efficient assembly of C9–C21 fragment **180**.

Synthesis of the second fragment **179** (Scheme 30) started out from dioxolanone **181**, derived from (*S*)-lactate,<sup>80</sup> which underwent enolate alkylation to install the C6 stereocentre in **188**. This was manipulated to provide propyl ketone **189**, which underwent a substrate-controlled, lithium-mediated aldol reaction with the DMB ether-containing aldehyde **190**, to afford *syn* adduct **191**. This was followed by PMBM (4-methoxybenzyloxymethyl) ether



**Scheme 30** Synthesis of alkenes **179** and **180**.

formation under mild conditions. This somewhat unusual choice of benzylic protecting group reconciled the earlier failure of a more conventional route, based on a PMB ether transposition.



**Scheme 31** RCM and completion of the total synthesis of actinoallolide A (**178**).



After selective DMB ether cleavage to give **192**, oxidation then completed the construction of acid **179**.

Ahead of embarking on the risky RCM manoeuvre, fragment union (Scheme 31) between **179** and **180** was accomplished by Yamaguchi esterification. In the absence of any plan B, it was an immense relief that extended treatment (over seven days!) with Hoveyda–Grubbs II catalyst in refluxing toluene was found to cleanly promote cyclisation to provide the required *E*-alkene in the 12-membered macrolactone **193**. Notably, this remarkable RCM reaction constitutes the most complex example to form a trisubstituted alkene in a medium-sized ring.<sup>81</sup> In the endgame, this key macrocycle **193** was then elaborated into triketone **194**, which underwent controlled desilylation and hemiacetalisation to complete the first total synthesis of (+)-actinoallolide A (**178**) in 20 steps LLS and 8% yield. The other four members of the actinoallolide family were readily prepared by late-stage diversification from **178**. Leveraging this expedient endgame, a photoaffinity probe was also designed and synthesised,<sup>82</sup> with a view to identifying the actinoallolide protein-binding target and mechanism of action.

## 4. Conclusions and perspectives

Spanning more than three decades of research, our group has achieved the total synthesis of over 40 distinct families of bioactive marine and terrestrial polyketide natural products. Throughout this challenging yet rewarding enterprise, we have demonstrated that chemists can emulate the sophisticated stereochemical control and modularity of the polyketide synthase biosynthetic machinery. In this context, the boron-mediated aldol reactions of chiral ethyl and methyl ketones with aldehydes are showcased in efficiently constructing a selection of densely oxygenated macrocyclic systems, ranging in ring size from 12- to 44-membered. Furthermore, the stereoinduction can be fine-tuned using the directing influence of *Ip*c ligands on the intermediate enolate. The reliability of these methods is further demonstrated through their varied applications in the stereocontrolled construction and coupling of large and small fragments. In conjunction with the controlled 1,3-*syn* or 1,3-*anti* reduction of the resulting  $\beta$ -hydroxyketones, this powerful aldol platform enables the rapid generation of stereochemical complexity and oxygenation to help unlock nature's polyketide treasure trove.

The synthetic methodology inspired by these exquisite polyketide architectures is exemplified by its application to the six macrolides covered in this article, and was first validated by the pioneering total synthesis of swinholide A. This demonstrated that carefully choreographed aldol reactions of ketones can be an effective tool to not only forge carbon–carbon bonds, but at the same time install stereocentres in a highly selective manner. Notably, the total synthesis of spongistatin 1 constitutes one of the most complex demonstrations of the utility, high efficiency and excellent levels of stereocontrol afforded by boron-mediated aldol methodology. Looking back on the serendipitous journey towards spirastrellolide, we were incredibly lucky in accidentally removing what transpired to be a problematic TES ether before

the macrolactonisation step, which only became apparent in the second-generation endgame. The total synthesis of leiodermatolide relied on flexible planning, combined with a series of highly stereocontrolled aldol reactions, efficient fragment couplings and careful tactical endgame manoeuvres for eventual success. The chivosazole campaign provided a painful reminder that complex polyene regions need to be viewed with caution when planning a synthesis. Once installed,  $sp^3$ -stereocentres can generally be depended on to retain their configuration. In contrast, the potential shapeshifting behaviour of conjugated alkenes can be much less predictable. As a bookend project, the actinoallolide synthesis was achieved by a single intrepid student, accomplishing the “do or die” RCM manoeuvre through sheer determination and perseverance.

On a more fundamental level, the challenging pursuit of these macrolide targets revealed so much more of the inherent chemical nature of these intriguing compounds than could ever be conjectured by pen and paper or thought experiments. Moreover, the new knowledge gained from embarking on their total synthesis reinforces the symbiotic relationship between synthetic and natural product isolation chemists, further enriching our collective understanding of these intriguing compounds.

Though not highlighted in this article, the group's versatile aldol methodology has also enabled the progression of polyketide drug candidates into clinical trials, as exemplified by the landmark Novartis large-scale total synthesis of discodermolide.<sup>83</sup> These trials, tribulations and serendipitous discoveries underscore how much we still have to learn to engineer precise molecular manipulations, especially when faced with such a dazzling array of functionalities that exemplify these and other natural product targets. Despite all this, the remarkable total syntheses of swinholide A, spongistatin 1, spirastrellolide A methyl ester, leiodermatolide, chivosazole F and actinoallolide A demonstrate how far we have progressed.

In closing, it is a pleasure to warmly thank the natural product groups that have discovered these fascinating macrolides, keeping us gainfully employed and intellectually challenged throughout. Without their timely bioprospecting activities and structural elucidation work, we would not have been able to embark on these and other equally memorable synthetic adventures.

## Conflicts of interest

There are no conflicts to declare.

## Acknowledgements

The work summarised in this Feature Article encompasses over 30 years of research, enabled by a total of 94 highly talented doctoral students and 60 postdocs at Cambridge. Their dedication, insight, perseverance and creative contributions are gratefully acknowledged. We thank the Woolf Fisher Trust (scholarship to NYSL) and the Herchel Smith Fund (scholarship to TPS and MJA) for support.



## Notes and references

- 1 I. Paterson and E. A. Anderson, *Science*, 2005, **310**, 451–453.
- 2 For the first part of this personal retrospective, see: T. P. Stockdale, N. Y. S. Lam, M. J. Anketell and I. Paterson, *Bull. Chem. Soc. Jpn.*, 2021, **94**, 713–731.
- 3 I. Paterson, *Pure Appl. Chem.*, 1992, **64**, 1821–1830.
- 4 A. Bernardi, C. Gennari, J. M. Goodman and I. Paterson, *Tetrahedron: Asymmetry*, 1995, **6**, 2613–2636.
- 5 (a) K.-M. Chen, G. E. Hardtmann, K. Prasad, O. Repič and M. J. Shapiro, *Tetrahedron Lett.*, 1987, **28**, 155–158; (b) D. A. Evans, K. T. Chapman and E. M. Carreira, *J. Am. Chem. Soc.*, 1988, **110**, 3560–3578; (c) D. A. Evans and A. H. Hoveyda, *J. Am. Chem. Soc.*, 1990, **112**, 6447–6449.
- 6 (a) C. J. Cowden and I. Paterson, *Organic Reactions*, ed. L. A. Paquette, Wiley, vol. 51, pp. 1–200, 1997; (b) I. Paterson, V. A. Doughty, G. J. Florence, K. Gerlach, M. D. McLeod, J. P. Scott and T. Trieselmann, in *Organoboranes for Syntheses*, ed. P. V. Ramachandran and H. C. Brown, American Chemical Society, ACS Symposium Series 783, ch. 14, pp. 195–206, 2001; (c) I. Paterson, C. J. Cowden and D. J. Wallace, in *Modern Carbonyl Chemistry*, ed. J. Otera, Wiley-VCH, 2000, pp. 249–297.
- 7 I. Paterson, J. M. Goodman, M. A. Lister, R. C. Schumann, C. K. McClure and R. D. Norcross, *Tetrahedron*, 1990, **46**, 4663–4684.
- 8 I. Paterson, J. M. Goodman and M. Isaka, *Tetrahedron Lett.*, 1989, **30**, 7121–7124.
- 9 (a) I. Paterson, D. J. Wallace and S. M. Velázquez, *Tetrahedron Lett.*, 1994, **35**, 9083–9086; (b) I. Paterson and D. J. Wallace, *Tetrahedron Lett.*, 1994, **35**, 9087–9090; (c) I. Paterson, D. J. Wallace and C. J. Cowden, *Synthesis*, 1998, 639–652.
- 10 (a) I. Paterson, M. A. Lister and C. K. McClure, *Tetrahedron Lett.*, 1986, **27**, 4787–4790; (b) I. Paterson and M. A. Lister, *Tetrahedron Lett.*, 1988, **29**, 585–588; (c) I. Paterson and J. M. Goodman, *Tetrahedron Lett.*, 1989, **30**, 997–1000.
- 11 S. Carmely and Y. Kashman, *Tetrahedron Lett.*, 1985, **26**, 511–514.
- 12 M. Kobayashi, J. Tanaka, T. Katori, M. Matsuura, M. Yamashita and I. Kitagawa, *Chem. Pharm. Bull.*, 1990, **38**, 2409–2418.
- 13 M. Kobayashi, K. Kawazoe, T. Okamoto, T. Sasaki and I. Kitagawa, *Chem. Pharm. Bull.*, 1994, **42**, 19–26.
- 14 M. R. Bubb, I. Spector, A. D. Bershadsky and E. D. Korn, *J. Biol. Chem.*, 1995, **270**, 3463–3466.
- 15 (a) C. A. Bewley, N. D. Holland and D. J. Faulkner, *Experientia*, 1996, **52**, 716–722; (b) J. Kobayashi and M. Ishibashi, *Chem. Rev.*, 1993, **93**, 1753–1769.
- 16 For other completed total syntheses, see: (a) K. C. Nicolaou, K. Ajito, A. P. Patron, H. Khatuya, P. K. Richter and P. Bertinato, *J. Am. Chem. Soc.*, 1996, **118**, 3059–3060; (b) K. C. Nicolaou, A. P. Patron, K. Ajito, P. K. Richter, H. Khatuya, P. Bertinato, R. A. Miller and M. J. Tomaszewski, *Chem. – Eur. J.*, 1996, **2**, 847–868; (c) I. Shin, S. Hong and M. J. Krische, *J. Am. Chem. Soc.*, 2016, **138**, 14246–14249.
- 17 (a) I. Paterson and J. D. Smith, *Tetrahedron Lett.*, 1993, **34**, 5351–5354; (b) I. Paterson and S. A. Osborne, *Tetrahedron Lett.*, 1990, **31**, 2213–2216.
- 18 I. Paterson and J. D. Smith, *J. Org. Chem.*, 1992, **57**, 3261–3264.
- 19 I. Paterson and J. G. Cumming, *Tetrahedron Lett.*, 1992, **33**, 2847–2850.
- 20 I. Paterson, J. G. Cumming, J. D. Smith and R. A. Ward, *Tetrahedron Lett.*, 1994, **35**, 441–444.
- 21 I. Paterson, J. D. Smith, R. A. Ward and J. G. Cumming, *J. Am. Chem. Soc.*, 1994, **116**, 2615–2616.
- 22 I. Paterson, J. G. Cumming, J. D. Smith, R. A. Ward and K.-S. Yeung, *Tetrahedron Lett.*, 1994, **35**, 3405–3408.
- 23 I. Paterson, K.-S. Yeung, R. A. Ward, J. G. Cumming and J. D. Smith, *J. Am. Chem. Soc.*, 1994, **116**, 9391–9392.
- 24 (a) I. Paterson, J. G. Cumming, R. A. Ward and S. Lamboley, *Tetrahedron*, 1995, **51**, 9393–9412; (b) I. Paterson, J. D. Smith and R. A. Ward, *Tetrahedron*, 1995, **51**, 9413–9436; (c) I. Paterson, R. A. Ward, J. D. Smith, J. G. Cumming and K. S. Yeung, *Tetrahedron*, 1995, **51**, 9437–9466; (d) I. Paterson, K.-S. Yeung, R. A. Ward, J. D. Smith, J. G. Cumming and S. Lamboley, *Tetrahedron*, 1995, **51**, 9467–9486.
- 25 (a) G. R. Pettit, Z. A. Chicacz, F. Gao, C. L. Herald, M. R. Boyd, J. M. Schmidt and J. N. A. Hooper, *J. Org. Chem.*, 1993, **58**, 1302–1304; (b) G. R. Pettit, Z. A. Chicacz, F. Gao, C. L. Herald and M. R. Boyd, *J. Chem. Soc., Chem. Commun.*, 1993, 1166–1168.
- 26 (a) M. Kobayashi, S. Aoki, H. Sakai, K. Kawazoe, N. Kihara, T. Sasaki and I. Kitagawa, *Tetrahedron Lett.*, 1993, **34**, 2795–2798; (b) M. Kobayashi, S. Aoki, H. Sakai, N. Kihara, T. Sasaki and I. Kitagawa, *Chem. Pharm. Bull.*, 1993, **41**, 989–991; (c) M. Kobayashi, S. Aoki and I. Kitagawa, *Tetrahedron Lett.*, 1994, **35**, 1243–1246; (d) M. Kobayashi, S. Aoki, K. Gato and I. Kitagawa, *Chem. Pharm. Bull.*, 1996, **44**, 2142–2149.
- 27 N. Fusetani, K. Shinoda and S. Matsunaga, *J. Am. Chem. Soc.*, 1993, **115**, 3977–3981.
- 28 (a) D. A. Evans, P. J. Coleman and L. C. Dias, *Angew. Chem., Int. Ed. Engl.*, 1997, **36**, 2738–2741; (b) D. A. Evans, B. W. Trotter, B. Côté and P. J. Coleman, *Angew. Chem., Int. Ed. Engl.*, 1997, **36**, 2741–2744; (c) D. A. Evans, B. W. Trotter, B. Côté, P. J. Coleman, L. C. Dias and A. N. Tyler, *Angew. Chem., Int. Ed. Engl.*, 1997, **36**, 2744–2747.
- 29 (a) J. Guo, K. J. Duffy, K. L. Stevens, P. I. Dalko, R. M. Roth, M. M. Hayward and Y. Kishi, *Angew. Chem., Int. Ed.*, 1998, **37**, 187–192; (b) M. M. Hayward, R. M. Roth, K. J. Duffy, P. I. Dalko, K. L. Stevens, J. Guo and Y. Kishi, *Angew. Chem., Int. Ed.*, 1998, **37**, 192–196.
- 30 R. K. Pettit, S. C. McAllister, G. R. Pettit, C. L. Herald, J. M. Johnson and Z. A. Chicacz, *Int. J. Antimicrob. Agents*, 1998, **9**, 147–152.
- 31 G. Menchon, A. E. Protá, D. Lucena-Agell, P. Bucher, R. Jansen, H. Irschik, R. Müller, I. Paterson, J. F. Díaz, K.-H. Altmann and M. O. Steinmetz, *Nat. Commun.*, 2018, **9**, 2106.
- 32 R. Bai, G. F. Taylor, Z. A. Chicacz, C. L. Herald, J. A. Kepler, G. R. Pettit and E. Hamel, *Biochemistry*, 1995, **34**, 9714–9721.
- 33 For other completed total syntheses, see: (a) A. B. Smith III, Q. Y. Lin, V. A. Doughty, L. H. Zhuang, M. D. McBriar, J. K. Kerns, A. M. Boldi, N. Murase, W. H. Moser, C. S. Brook, C. S. Bennett, K. Nakayama, M. Sobukawa and R. E. Trout, *Tetrahedron*, 2009, **65**, 6470–6488; (b) A. B. Smith III, C. Sfougataki, C. A. Risatti, J. B. Sperry, W. Y. Zhu, V. A. Doughty, T. Tomioka, D. B. Gotchev, C. S. Bennett, S. Sakamoto, O. Atasoylu, S. Shirakami, D. Bauer, M. Takeuchi, J. Koyanagi and Y. Sakamoto, *Tetrahedron*, 2009, **65**, 6489–6509; (c) C. H. Heathcock, M. McLaughlin, J. Medina, J. L. Hubbs, G. A. Wallace, R. Scott, M. M. Claffey and C. J. Hayes, *J. Am. Chem. Soc.*, 2003, **125**, 12844–12849; (d) M. T. Crimmins, J. D. Katz, D. G. Washburn, S. P. Allwein and L. F. McAtee, *J. Am. Chem. Soc.*, 2002, **124**, 5661–5663; (e) M. Ball, M. J. Gaunt, D. F. Hook, A. S. Jessiman, S. Kawahara, P. Orsini, A. Scolaro, A. C. Talbot, H. R. Tanner, S. Yamanoi and S. V. Ley, *Angew. Chem., Int. Ed.*, 2005, **44**, 5433–5438; (f) L. M. Suen, M. A. Tekle-Smith, K. S. Williamson, J. R. Infantine, S. K. Reznik, P. S. Tanis, T. D. Casselman, D. L. Sackett and J. L. Leighton, *Nat. Commun.*, 2018, **9**, 4710.
- 34 I. Paterson, D. Y.-K. Chen, M. J. Coster, J. L. Acena, J. Bach, K. R. Gibson, L. E. Keown, R. M. Oballa, T. Trieselmann, D. J. Wallace, A. Hodgson and R. D. Norcross, *Angew. Chem., Int. Ed.*, 2001, **40**, 4055–4060.
- 35 (a) I. Paterson and R. M. Oballa, *Tetrahedron Lett.*, 1997, **38**, 8241–8244; (b) I. Paterson, M. J. Coster, D. Y.-K. Chen, R. M. Oballa, D. J. Wallace and R. D. Norcross, *Org. Biomol. Chem.*, 2005, **3**, 2399–2409.
- 36 (a) I. Paterson, K. R. Gibson and R. M. Oballa, *Tetrahedron Lett.*, 1996, **37**, 8585–8588; (b) I. Paterson and L. A. Collett, *Tetrahedron Lett.*, 2001, **42**, 1187–1191; (c) D. A. Evans, P. J. Coleman and B. Côté, *J. Org. Chem.*, 1997, **62**, 788–789; (d) D. A. Evans, B. Côté, P. J. Coleman and B. T. Connell, *J. Am. Chem. Soc.*, 2003, **125**, 10893–10898.
- 37 (a) I. Paterson, D. J. Wallace and K. R. Gibson, *Tetrahedron Lett.*, 1997, **38**, 8911–8914; (b) I. Paterson and M. J. Coster, *Tetrahedron Lett.*, 2002, **43**, 3285–3289; (c) I. Paterson, M. J. Coster, D. Y. K. Chen, K. R. Gibson and D. J. Wallace, *Org. Biomol. Chem.*, 2005, **3**, 2410–2419.
- 38 I. Paterson, M. J. Coster, D. Y. K. Chen, J. L. Aceña, J. Bach, L. E. Keown and T. Trieselmann, *Org. Biomol. Chem.*, 2005, **3**, 2420–2430.
- 39 H. C. Kolb, M. S. VanNieuwenhze and K. B. Sharpless, *Chem. Rev.*, 1994, **94**, 2483–2547.
- 40 I. Paterson, K.-S. Yeung and J. B. Smail, *Synlett*, 1993, 774–776.
- 41 I. Paterson, D. Y. K. Chen, M. J. Coster, J. L. Aceña, J. Bach and D. J. Wallace, *Org. Biomol. Chem.*, 2005, **3**, 2431–2440.



- 42 D. A. Evans, B. W. Trotter, P. J. Coleman, B. Côté, L. C. Dias, H. A. Rajapakse and A. N. Tyler, *Tetrahedron*, 1999, **55**, 8671–8726.
- 43 I. Paterson, J. L. Acena, J. Bach, D. Y.-K. Chen and M. J. Coster, *Chem. Commun.*, 2003, 462–463.
- 44 D. E. Williams, M. Roberge, R. Van Soest and R. J. Andersen, *J. Am. Chem. Soc.*, 2003, **125**, 5296–5297.
- 45 D. E. Williams, M. Lapawa, X. Feng, T. Tarling, M. Roberge and R. J. Andersen, *Org. Lett.*, 2004, **6**, 2607–2610.
- 46 (a) I. Paterson, E. A. Anderson, S. M. Dalby, J. H. Lim, J. Genovino, P. Maltas and C. Moessner, *Angew. Chem., Int. Ed.*, 2008, **47**, 3016–3020; (b) I. Paterson, E. A. Anderson, S. M. Dalby, J. H. Lim, J. Genovino, P. Maltas and C. Moessner, *Angew. Chem., Int. Ed.*, 2008, **47**, 3021–3025; (c) I. Paterson, P. Maltas and E. A. Anderson, *Pure Appl. Chem.*, 2013, **85**, 1133–1147.
- 47 I. Paterson, P. Maltas, S. M. Dalby, J. H. Lim and E. A. Anderson, *Angew. Chem., Int. Ed.*, 2012, **51**, 2749–2753.
- 48 For other completed total syntheses, see: (a) G. W. O'Neil, J. Ceccon, S. Benson, M.-P. Collin, B. Fasching and A. Fürstner, *Angew. Chem., Int. Ed.*, 2009, **48**, 9940–9945; (b) S. Benson, M.-P. Collin, G. W. O'Neil, J. Ceccon, B. Fasching, M. D. B. Fenster, C. Godbout, K. Radkowski, R. Goddard and A. Fürstner, *Angew. Chem., Int. Ed.*, 2009, **48**, 9946–9950; (c) S. Benson, M.-P. Collin, A. Arlt, B. Gabor, R. Goddard and A. Fürstner, *Angew. Chem., Int. Ed.*, 2011, **50**, 8739–8744.
- 49 I. Paterson, E. A. Anderson, S. M. Dalby, J. H. Lim, P. Maltas, O. Loiseleur, J. Genovino and C. Moessner, *Org. Biomol. Chem.*, 2012, **10**, 5861–5872.
- 50 I. Paterson, E. A. Anderson, S. M. Dalby, J. H. Lim and P. Maltas, *Org. Biomol. Chem.*, 2012, **10**, 5873–5886.
- 51 I. Paterson, E. A. Anderson, S. M. Dalby and O. Loiseleur, *Org. Lett.*, 2005, **7**, 4121–4124.
- 52 I. Paterson, E. A. Anderson, S. M. Dalby and O. Loiseleur, *Org. Lett.*, 2005, **7**, 4125–4128.
- 53 I. Paterson, E. A. Anderson and S. M. Dalby, *Synthesis*, 2005, 3225–3228.
- 54 I. Paterson, E. A. Anderson, S. M. Dalby, J. H. Lim, P. Maltas and C. Moessner, *Chem. Commun.*, 2006, 4186–4188.
- 55 I. Paterson, E. A. Anderson, S. M. Dalby, J. Genovino, J. H. Lim and C. Moessner, *Chem. Commun.*, 2007, 1852–1854.
- 56 S. Hu, S. Jayaraman and A. C. Oehlschlager, *J. Org. Chem.*, 1996, **61**, 7513–7520.
- 57 I. Paterson and S. M. Dalby, *Nat. Prod. Rep.*, 2009, **26**, 865–873.
- 58 A. E. Wright, J. K. Reed, J. Roberts and R. E. Longley, *US Pat.*, US2008033035 (*Chem. Abstr.*, 2008, 148, 230103).
- 59 I. Paterson, S. M. Dalby, J. C. Roberts, G. J. Naylor, E. A. Guzmán, R. Isbrucker, T. P. Pitts, P. Linley, D. Divlianska, J. K. Reed and A. E. Wright, *Angew. Chem., Int. Ed.*, 2011, **50**, 3219–3223.
- 60 I. Paterson, T. Paquet and S. M. Dalby, *Org. Lett.*, 2011, **13**, 4398–4401.
- 61 I. Paterson and S. Williams, *Isr. J. Chem.*, 2017, **57**, 192–201.
- 62 (a) J. Willwacher, N. Kausch-Busies and A. Fürstner, *Angew. Chem., Int. Ed.*, 2012, **51**, 12041–12046; (b) D. Mailhol, J. Willwacher, N. Kausch-Busies, E. E. Rubitski, Z. Sobol, M. Schuler, M. H. Lam, S. Musto, F. Loganzo, A. Maderna and A. Fürstner, *J. Am. Chem. Soc.*, 2014, **136**, 15719–15729.
- 63 I. Paterson, K. K. H. Ng, S. Williams, D. C. Millican and S. M. Dalby, *Angew. Chem., Int. Ed.*, 2014, **53**, 2692–2695.
- 64 R. Jansen, H. Irschik, H. Reichenbach and G. Höfle, *Liebigs Ann.*, 1997, 1725–1732.
- 65 D. Janssen, D. Albert, R. Jansen, R. Müller and M. Kalesse, *Angew. Chem., Int. Ed.*, 2007, **46**, 4898–4901.
- 66 T. Brodmann, D. Janssen and M. Kalesse, *J. Am. Chem. Soc.*, 2010, **132**, 13610–13611.
- 67 S. Williams, K. Jin, S. B. J. Kan, M. Li, L. J. Gibson and I. Paterson, *Angew. Chem., Int. Ed.*, 2017, **56**, 645–649.
- 68 I. Paterson, S. B. J. Kan and L. J. Gibson, *Org. Lett.*, 2010, **12**, 3724–3727.
- 69 S. I. Shirokawa, M. Kamiyama, T. Nakamura, M. Okada, A. Nakazaki, S. Hosokawa and S. Kobayashi, *J. Am. Chem. Soc.*, 2004, **126**, 13604–13605.
- 70 J. Uenishi, R. Kawahama, O. Yonemitsu and J. Tsuji, *J. Org. Chem.*, 1998, **63**, 8965–8975.
- 71 G. Stork and K. Zhao, *Tetrahedron Lett.*, 1989, **30**, 2173–2174.
- 72 I. Paterson, L. J. Gibson and S. B. J. Kan, *Org. Lett.*, 2010, **12**, 5530–5533.
- 73 W. C. Still and C. Gennari, *Tetrahedron Lett.*, 1983, **24**, 4405–4408.
- 74 Y. Inahashi, M. Iwatsuki, A. Ishiyama, A. Matsumoto, T. Hirose, J. Oshita, T. Sunazuka, W. Panbangred, Y. Takahashi, M. Kaiser, K. Otoguro and S. Omura, *Org. Lett.*, 2015, **17**, 864–867.
- 75 M. J. Anketell, T. M. Sharrock and I. Paterson, *Angew. Chem., Int. Ed.*, 2020, **59**, 1572–1576.
- 76 D. Seebach, R. Naef and G. Calderari, *Tetrahedron*, 1984, **40**, 1313–1324.
- 77 (a) I. Paterson and A. N. Hulme, *Tetrahedron Lett.*, 1990, **31**, 7513–7516; (b) I. Paterson and A. N. Hulme, *J. Org. Chem.*, 1995, **60**, 3288–3300.
- 78 J. G. Solsona, J. Nebot, P. Romea and F. Urpí, *J. Org. Chem.*, 2005, **70**, 6533–6536.
- 79 J. Esteve, S. Matas, M. Pellicena, J. Velasco, P. Romea, F. Urpí and M. Font-Bardia, *Eur. J. Org. Chem.*, 2010, 3146–3151.
- 80 R. Nagase, Y. Oguni, T. Misaki and Y. Tanabe, *Synthesis*, 2006, 3915–3917.
- 81 C. Lecourt, S. Dhambri, L. Allievi, Y. Sanogo, N. Zeghib, R. B. Othman, M.-I. Lannou, G. Sorin and J. Ardisson, *Nat. Prod. Rep.*, 2018, **35**, 105–124.
- 82 M. J. Anketell, T. M. Sharrock and I. Paterson, *Org. Biomol. Chem.*, 2020, **18**, 8109–8118.
- 83 (a) S. J. Mickel, D. Niederer, R. Daeffler, A. Osani, E. Kuesters, E. Schmid, K. Schaer, R. Gamboni, W. Chen, E. Loeser, F. R. Kinder, K. Königsberger, K. Prasad, T. M. Ramsey, O. Repic, R.-M. Wang, G. Florence, I. Lyothier and I. Paterson, *Org. Process Res. Dev.*, 2004, 122–130; (b) G. J. Florence, N. M. Gardner and I. Paterson, *Nat. Prod. Rep.*, 2008, **25**, 342–375.

